Master dissertation

Inatel
Instituto Nacional de Telecomunicações

Optically-powered Hybrid RoF/VLC Systems for 6G Applications

Felipe Batista Faro Pinto

February/2024

OPTICALLY-POWERED HYBRID ROF/VLC SYSTEMS FOR 6G APPLICATIONS

FELIPE BATISTA FARO PINTO

Master's dissertation presented at National Institute of Telecommunications (Inatel), as part of the requirements for obtaining the Master's Degree in Telecommunication Engineering.

ADVISOR: Prof. Dr. Arismar Cerqueira Sodré Junior.

CO-ADVISOR: Dr. Eduardo Saia Lima.

Santa Rita do Sapucaí-MG
2024

Pinto, Felipe Batista Faro.
P658o
Optically-powered Hybrid RoF/VLC Systems for 6G Applications / Felipe Batista Faro Pinto – Santa Rita do Sapucaí, 2024.
77 p.

Orientadores: Prof. Dr. Arismar Cerqueira Sodré Junior/ Dr. Eduardo Saia Lima.
Dissertação de Mestrado em Telecomunicações – Instituto Nacional de Telecomunicações – INATEL.
Inclui bibliografia.

1. 5G/6G 2. Multimode fiber 3. Power-over-fiber 4. radio-over-fiber 5. Visible light communication 6. Mestrado em Telecomunicações. I. Sodré Junior, Arismar Cerqueira II. Lima, Eduardo Saia III. Instituto Nacional de Telecomunicações – INATEL. IV. Título.

CDU 621.39

Ficha Catalográfica elaborada pelo Bibliotecário da Instituição
CRB6-2718 – Paulo Eduardo de Almeida

APPROVAL FORM

Dissertation defended and approved in February 1th, 2024 by the judging committee:

Prof. Dr. José Antônio Justino Ribeiro

Prof. Dr. Rômulo Mota Volpato

Prof. Dr. Arismar Cerqueira Sodré Junior
Instituto Nacional de Telecomunicações (Inatel)

Graduate Course Coordinator
Prof. Dr. José Marcos Camara Brito

To my family and friends,
for the patience, guidance and support.

Acknowledgments

First, I would like to express my heartfelt gratitude to my family, my pillar of strength throughout this academic journey. To my parents, Gabriel and Ana Lúcia, whose unwavering support and encouragement have been my guiding light. Your sacrifices and belief in my abilities have been instrumental in reaching this significant achievement. My siblings, Lorena and Bernardo, thank you for the real friendship and love, you are and always will be a constant source of inspiration. I love you all!

I want to express my sincere thanks to my esteemed advisor Arismar Cerqueira Sodré Junior for your invaluable guidance, mentorship, and, of course, for the opportunity to work with him in the laboratory WOCA. I am also thankful for my co-advisor and friend, Dr. Eduardo Saia Lima. Thank you for accepting this challenge to co-adviser me in this journey. Your expertise, patience, and commitment played an essential role in shaping the trajectory of my research.

I extend my sincere thanks to all my friends and colleagues from laboratory WOCA, who made this research journey a collaborative and enriching experience. Your friendship, shared insights, and mutual support have not only made the work more enjoyable but have also contributed significantly to the depth and quality of the outcomes.

Finally, I would also like to thank the National Institute of Telecommunication Foundation (FINATEL) and the Research Support Foundation of the State of Minas Gerais (FAPEMIG) for the scholarship. This work was partially supported by RNP, with resources from MCTIC, Grant No. 01245.020548/2021-07, under the Brazil 6G project of the Radiocommunication Reference Center (CRR) of the National Institute of Telecommunications (Inatel), Brazil, and by Huawei, under the project Advanced Academic Education in Telecommunications Networks and Systems, contract No PPA6001BRA23032110257684. Thank the financial support from CNPq, CAPES, FINEP, FAPEMIG, FAPESP, and MPTcable.

Index

List of Figures

List of Tables

List of Acronyms

3GPP	3rd Generation Partnership Project
5G	Fifth generation of mobile networks
6G	Sixth generation of mobile networks
AD	Analog-to-digital
A-RoF	Analog Radio over Fiber
B2B	Building-to-building
BS	Base station
BT	Bias tee
CO	Central office
C-RAN	Centralized radio access network
DA	Digital-to-analog
DCF	Double-clad optical fiber
EDFA	Erbium-doped fiber amplifier
eMBB	Enhanced mobile broadband
EO	Electrical-to-optical
EVM_{RMS}	Root mean square error vector magnitude
FiWi	Fiber-Wireless
FR1	Frequency range 1
Gbps	Gigabits per second
HPLD	High-power laser diode
IIoT	Industrial Internet of Things
IoT	Internet of Things
KPI	Key performance indicators
laser	Light amplification by stimulated emission of radiation
LED	Light-emitting diode
MCF	Multicore optical fiber
MFD	Mode field diameter
MMF	Multimode optical fiber
mMTC	Massive machine-type communication
mmWave	Millimeter-Wave
MPP	Maximum power point
NR	New Radio
OE	Optical-to-electrical
OPTE	Optical power transmission efficiency
OWC	Optical wireless communication
PLC	Power line communications

PoE	Power-over-Ethernet
PoF	Power-over-Fiber
PPC	Photovoltaic power converter
PTE	Power transmission efficiency
QAM	Quadrature amplitude modulation
R2V	Road-to-vehicle
RF	Radio Frequency
RoF	Radio over Fiber
SBS	Stimulated Brillouin scattering
SFDR	Spurious-free dynamic range
SMF	Single-mode fiber
SNR	Signal-to-noise ratio
SRS	Stimulated Raman scattering
TEC	Thermoelectric cooler
URLLC	Ultra-reliable and low latency communications
V2V	Vehicle-to-vehicle
VLC	Visible Light Communication

List of Symbols

A_{eff}	Effective area
α	Fiber attenuation
b	Polarization factor
d_{mfd}	Fiber mode field diameter
g_{b}	Brillouin gain coefficient
g_{R}	Raman gain coefficient
I_{th}	Threshold power density
L	Fiber length
λ	Wavelength
L_{eff}	Effective fiber length
NA	Numerical aperture
P_{SBS}	SBS threshold power
P_{SRS}	SRS threshold power
P_{th}	Threshold power
r	Fiber radius
V	Fiber V number
Δv_{b}	Brillouin linewidth
Δv_{source}	Source linewidth
w	Core effective radius

Summary of Original Works

This dissertation is based on the following original publications:

(1) **Felipe Batista Faro Pinto**, Letícia Carneiro de Souza, Tomás Powell Villena Andrade, Eduardo Saia Lima, Luis Gustavo da Silva, Francisco Martins Portelinha Junior, Evandro Lee Anderson, Rodnei Carçola and Arismar Cerqueira Sodré Junior. "PoF System Using Standard 62.5-micron Multimode Fiber for 5G NR Industrial Applications", accepted in *20th SBMO/IEEE MTT-S International Microwave and Optoelectronics Conference (IMOC 2023)*, Barcelona, Espanha.

(2) **Felipe Batista Faro Pinto**, Letícia Carneiro de Souza, Tomás Powell Villena Andrade, Eduardo Saia Lima, Rodnei Carçola, Evandro Lee Anderson, Francisco Martins Portelinha Junior and Arismar Cerqueira Sodré Junior. "Optically-powered FiWi System for B5G Hybrid VLC/RF Access Networks", submitted in *Optics Express*.

Other scientific reports:

(3) **Felipe Batista Faro Pinto**, Pedro Arthur Bessa Leão and Arismar Cerqueira Sodré Junior. "Posicionador de Antenas Automatizado de Baixo Custo para Medições de Diagramas de Radiação", accepted in *XLI Simpósio Brasileiro de Telecomunicações e Processamento de Sinais*, São José dos Campos-SP.

Resumo

Esta dissertação apresenta a implementação de dois sistemas *Power-over-Fiber* (PoF) para prover energia elétrica opticamente a duas arquiteturas de comunicações móveis, sendo uma 5G e outra 6G. A primeira implementação baseia-se no uso de um sistema de rádio sobre fibra (*Radio over Fiber* ou RoF) com o padrão 5G *New Radio* (5G NR) em conjunto com PoF para ambientes industriais. O sinal 5G NR centrado em 3,5 GHz com 100 MHz de largura de faixa é transmitido ao longo de um enlace de fibra óptica monomodo (SMF) de 20 km. Em relação ao sistema PoF, uma potência óptica de 5 W é transmitida por meio de uma fibra óptica multimodo convencional (MMF) de 100 m, com diâmetro do núcleo de 62,5 μm, visando prover energia para um módulo RoF. Obtém-se uma eficiência de transmissão de energia (*Power Transmission Efficiency* ou PTE) de aproximadamente 19% e analisa-se o desempenho do sistema 5G NR utilizando a métrica EVM_{RMS} (*Root MEan Square Error Vector Magnitue*). Alcança-se uma vazão de 600 Mbps sem degradação significativa de desempenho em comparação ao sistema RoF alimentado convencionalmente, demonstrando a aplicabilidade e o potencial da técnica PoF para comunicações industriais baseadas em 5G NR. A segunda implementação é concernente a sistemas híbridos de comunicação por luz visível (*Visible Light Communication* ou VLC) e *Fiber-Wireless* (FiWi) alimentados opticamente voltados para redes 6G internas. O sistema PoF é capaz de energizar dois dispositivos, um módulo RoF, que contém um fotodetector e um amplificador de RF, e um laser VLC vermelho. Uma fibra MMF convencional de 500 m é utilizada para transportar uma potência óptica de 8,1 W, alcançando aproximadamente 1,06 W de potência elétrica e uma PTE de 14%. Já o sinal 5G NR gerado é transportado ao longo de um fronthaul de 10 km de fibra SMF, utilizando tecnologia RoF, antes de ser radiado por uma rede acesso híbrida com RF e luz visível. Demonstra-se uma vazão 1,2 Gbps no sistema VLC usando um sinal 5G NR com largura de faixa de 200 MHz e 64 QAM (*Quadrature Amplitude Modulation*), resultando em aproximadamente 4,02% de EVM_{RMS}. Por fim, mais uma comparação entre o sistema PoF e a alimentação elétrica convencional é realizada, validando o desempenho do sistema PoF e sua aplicabilidade para redes 5G/6G internas.

***Palavras-Chave*:** 5G, 6G, comunicação por luz visível, fibra multimodo, *power-over-fiber* e radio sobre fibra.

Abstract

This dissertation presents the implementation of two power-over-fiber (PoF) systems, aiming to optically feed two different architectures of 5G/6G networks. The first implementation is regarding the deployment of a radio-over-fiber (RoF)-based 5G New Radio (NR) system in conjunction with PoF for industrial environments. A 100 MHz bandwidth 5G NR signal centered at 3.5-GHz is transmitted throughout a 20-km single-mode optical fiber (SMF) link. Regarding the PoF system, a 5-W optical power is transmitted through a 100-m conventional multimode optical fiber (MMF) link with 62.5 μm core diameter, with the purpose of powering an RoF module. It achieves a PoF system power transmission efficiency (PTE) of around 19% and the 5G NR system performance is evaluated as a function of the root mean square error vector magnitude (EVM_{RMS}). A throughput of 600 Mbps is achieved with no performance degradation when compared to a conventional electrically-powered RoF system, demonstrating the applicability and potential of the PoF technique for 5G NR-based industrial communications. The second implementation relies on a hybrid optically-powered visible light communication (VLC) and fiber-wireless (FiWi) systems towards 6G indoor applications. The proposed PoF system is able to energize two loads, a RoF module, which contains a photodetector and an RF amplifier, and a VLC red laser. A 500 m conventional MMF link is used to transport 8.1 W optical power, obtaining approximately 1.06 W electrical power and a PTE of 14%. Regarding the communication link, a 5G NR signal is transmitted throughout a 10-km SMF fronthaul based on RoF technology, before being radiated in a hybrid access networks based on RF and VLC links. It is demonstrated a 1.2 Gbps throughput in the VLC link using a 5G NR signal with 200-MHz bandwidth and 64 quadrature amplitude modulation (QAM), resulting in approximately 4.02% EVM_{RMS}. Finally, another comparison between the PoF system and a conventional power supply is performed, validating the PoF system applicability for the 5G/6G indoor networks.

***Keywords*:** 5G, 6G, multimode fiber, power-over-fiber, radio-over-fiber and visible light communication.

Chapter 1

Introduction

1.1 Contextualization and Motivation

The increasing request for higher data rates, lower latency, higher reliability and energy efficiency, motivated the rapid advance in mobile communications technologies over the years. In this context, the fifth generation of mobile networks (5G) has been developed and commercialized worldwide as a rupture in the paradigm in relation to the previous generations, covering three application scenarios: enhanced mobile broadband (eMBB), reaching data rates up to 20 Gb/s in downlink; ultra-reliable and low latency communications (URLLC), providing latency lower than 1 ms; massive machine-type communication (mMTC), handling with up to 10^6 devices/km^2 [1–5]. At the same time, the sixth generation of mobile networks (6G) is already under study, envisaging the application scenarios and also the key features, such as high security and privacy, low energy consumption, and extremely large bandwidth compared with 5G [6–8]. Figure 1.1 reports the main key performance indicators (KPI) and also the use cases expected for the future 6G networks.

In order to achieve the 5G and 6G requirements, multiple techniques and technologies emerge with great potential to be implemented in mobile networks. Particularly, the radio over fiber (RoF) technique, which consists of transmitting radio frequency (RF) signals by means of an optical fiber. RoF is an essential technology due to the high bandwidth available, enabling the transmission of high data rates, in addition to a lower attenuation than the coaxial cables, reaching longer distances or allowing to reduce the required transmission power of the system [10–13]. Aiming to simplify the base station (BS) and reduce it is energy consumption, analog radio over fiber (A-RoF), which transmits the RF signals already in the interest frequency throughout the optical-fiber link, might be implemented in the 6G transport network, by applying centralized

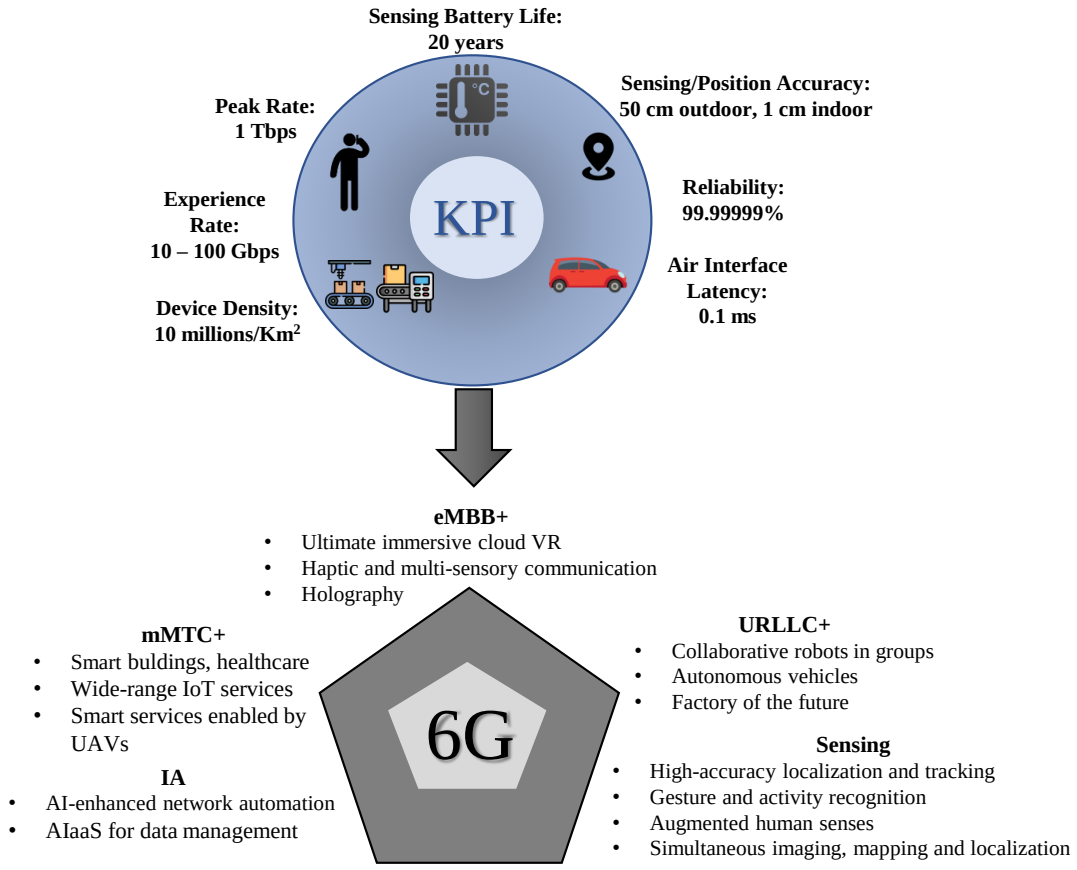

Figure 1.1: *KPI and use cases for the future 6G networks. Adapted from [9].*

radio access network (C-RAN) architecture for the mobile network infrastructure [14]. The C-RAN architecture consists in centralizing all the baseband processed signals at the central office (CO) [15]. By using A-RoF in an optical fronthaul in order to connect the CO to the BS, some costs are eliminated in the BS, such as digital-to-analog (DA) conversions and frequency upconversion for the downlink and analog-to-digital (AD) conversions and frequency downconversion for the uplink [16].

Regarding the access network, an RF wireless system is the more common approach to attend to the plethora of users, which combined with an optical fronthaul composes a fiber-wireless (FiWi) system. Nevertheless, other technologies have emerged as an alternative to complement the conventional antennas. The visible light communication (VLC) is a type of optical wireless communication (OWC) and appears with great potential for the 6G networks by offering not only data transmission using visible light, but also illumination for indoor environments, becoming an interesting option to bring high throughput and security to users [17]. In addition to these advantages, VLC operates in an unlicensed spectrum, providing a larger bandwidth than the millimeter-wave (mmWave), and also has interference immunity to the RF signals present in the environment [18, 19]. However, due to the interference caused by solar

radiation, this technology is more suitable for indoor applications and indicated for environments sensitive to electromagnetic waves, such as hospitals, industry, and airplanes [17, 20]. Nevertheless, VLC is also implemented in outdoor scenarios such as vehicle-to-vehicle (V2V), road-to-vehicle (R2V), and even building-to-building (B2B) communications [21], by using some techniques as a machine learning-based adaptive filter [22], a differential filtering-based receiver [23], and a bandpass optical blue filter [24], in order to mitigate the problems due the sunlight interference.

With regards to power distribution, certain technologies enable the transportation of data and power through the same medium. Power line communications (PLC) utilizes existing copper power lines to embed data, thereby providing both electric energy and communication simultaneously. Designed for the ”last mile,” PLC has some limitations, such as noise and attenuation, which increase with carrier frequency, thus restricting bandwidth and throughput [25, 26]. Another technology, known as power-over-ethernet (PoE), has emerged as a highly effective low-cost solution for enabling data and power transmission through a single Ethernet cable [27]. With the IEEE 802.3bt standard, PoE can deliver up to 99 W, limited to distances less than 100 m [28, 29].

In this context, power-over-fiber (PoF) technology could be considered a promising approach to optically power 5G/6G networks, including femtocells operating in mmWave. PoF consists of transmitting high optical power levels (order of tens of Watts) through fiber-optics links, with the purpose of feeding low-power consumption components generally from remote areas and/or hazardous environments. In general terms, a PoF system comprises a high-power laser diode (HPLD), which provides high optical power to the system, an optical fiber, and a photovoltaic power converter (PPC), which converts the optical power to electrical power. PoF system has several advantages over the use of cooper wires, such as low loss (reaching longer distances than PLC and PoE), electromagnetic interference immunity, low weight, and galvanic isolation [30]. These characteristics make the PoF an excellent solution to supply components placed in mines, factories, underwater conditions, and other harsh environments. Figure 1.2 reports a generic PoF system and also a scenario of an optically-powered 5G/6G network applied to an industrial environment. This application scenario becomes interesting for PoF since one of the challenges in an industrial environment is the electromagnetic interference and also, depending on the type of manufacturing, there may be flammable gases in the air. Therefore, the use of copper wires to supply electrical power to devices could not be the best solution on the factory floor [31]. In this context, PoF systems have been showing a huge potential to complement the use of cooper wires, due to all the advantages of an optical fiber [32]. However, there are

challenges to improving the feasibility of a PoF system. For example, the conversion efficiency of a commercial PPC is still low, providing values around 24% with a maximum input power of 10 W [33]. Consequently, this process needs to be enhanced in order to improve the total efficiency of the system.

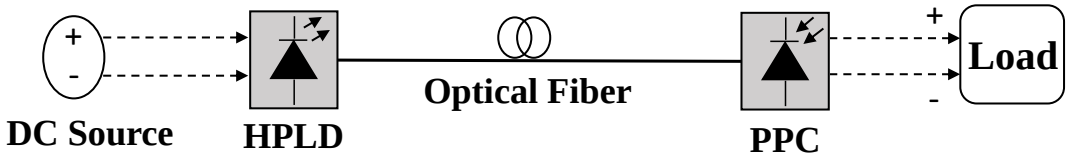

(a) *Generic PoF system.*

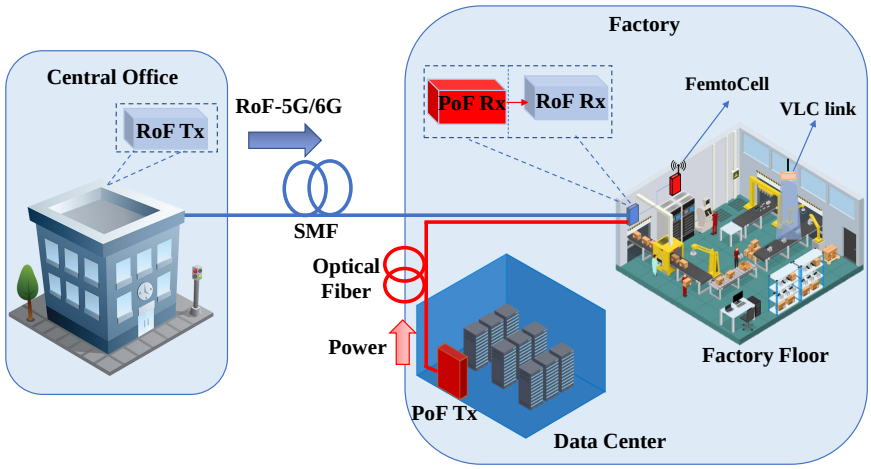

(b) *Optically-powered C-RAN and RoF-based 5G/6G network applied to industrial environment.*

Figure 1.2: *PoF system and application scenario.*

1.2 Literature Review

Works in the literature have applied PoF in different scenarios with distinct types of optical fiber. The main optical fibers used in PoF systems are the single-mode fiber (SMF), multimode optical fiber (MMF), double-clad optical fiber (DCF), and multicore optical fiber (MCF). All these fiber structures are presented in Figure 1.3. For instance, in [34], the authors have implemented a PoF system using SMF to transmit power and data together, aiming for 5G network and Internet of Things (IoT) appli-

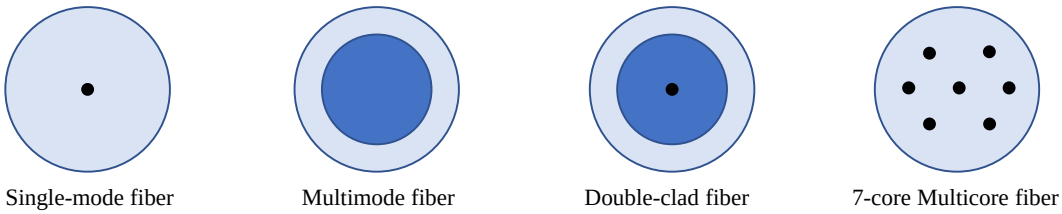

Figure 1.3: *Potential optical fibers to be used in PoF systems.*

cations. A 2 W optical power centered at 1480 nm was transmitted with a 5G New Radio (NR) signal over 10 km of a SMF, obtaining 870 mW at the end of the demultiplexer. In [35] was reported a co-transmission of 10 W optical power with a 5G NR signal throughout a 1 km SMF link, collecting 7.18 W of optical power at the end of the system. In [36], the authors have implemented a 14.43-km SMF link to transmit a 2.24-W optical power signal. Approximately 200 mW of electrical power was delivered, obtaining of 10% of power transmission efficiency (PTE). Moreover, PoF system using MMF is presented in [37–42]. In particular, our research group [37] have used 100 m MMF with 100 μm of core diameter in a dedicated link to transmit 2.2 W optical power in order to feed a RoF module applied in an SMF based-5G NR system. A dedicated 300 m MMF link with 200 μm of core diameter was used to transmit 1.5 W in [38]. 360 mW was obtained after the optical-to-electrical (OE) conversion, which was used to feed a proximity sensor for hazardous environment applications. In [39], a 4 km MMF link with 62.5 μm of core diameter was used in a shared scenario, by transmitting 10 W optical power and a 5G NR signal in the same MMF link. The center-launching and offset-launching techniques were used in order to mitigate the modal dispersion and crosstalk interference for the co-transmission, collecting 6 W of output optical power. Meanwhile, in [40], a 300 m MMF with 62.5 μm of core diameter was implemented to transmit 250 mw optical power, in order to feed a short-range remote unit. In [41], the authors presented a PoF system using a 100-m MMF with a 100-μm core diameter, transmitting 5 W of optical power, aiming at Industrial Internet of Things (IIoT) applications. A PoF system transmitting 1.5-W optical power through a 300-m MMF with 200-μm core diameter was reported in [42], aiming to supply smart remote nodes. In [43], a single 100 m-MMF has been implemented in order to transmit three types of signal (digital, RF, and power). As a result, an root mean square error vector magnitude (EVM_{RMS}) around 2% and a PTE of approximately 6% was achieved with this configuration. Whereas, in [44], a PoF-based system designed to power IoT sensors (temperature and humidity) using 300 m of MMF has been demonstrated. As a result, the authors achieved 279 mW of delivered electrical power with an efficiency of 16.5%. In [45], a 62.5 um MMF-based PoF for voltage, current, and temperature measurements in medium voltage distribution networks was employed, reaching 80 mW of electrical power, which was used to power a laser, electronic circuits, and sensors.

There are works that have explored special optical fibers as the DCF [46–49] and also the MCF [50–52], aiming for application in a shared scenario-based PoF systems, i.e., power and data transmission using a same fiber. In [46], 150 W optical power provided by 4 HPLD was injected in the inner clad of a 1 km DCF link and data was simultaneously transmitted in the 8 μm core. At the output of the six PPCs, was

obtained 7.08 W. The same authors, in [47], have used 2-W HPLDs and high-power photodetectors resulting in over 400 mW of delivered electrical power, whereas in [48], 60 W optical power was transmitted, obtaining 26 W output optical power. A DCF was also used in [49], in which a bidirectional communication system was carried out by transmitting data in the 9 μm core and 4 W optical power in the inner clad, collecting 400 mW at the output of the two PPCs. In [50], 60 W optical power provided by six HPLDs was co-transmitted with a 5G NR signal in a 1 km MCF link. By using six PPCs at the end of the PoF system, the authors achieved approximately 11.9 W. Whereas in [51], the authors reported a PoF-based 5G NR network employing RoF technology and a MCF link. A main board, basically composed of a microcontroller, was powered by the PoF system. An optically-powered RoF system employing a MCF link has been proposed [52]. A 12-gigabits per second (Gbps) signal with a central frequency of 92 GHz was simultaneously transmitted with a 0.8-W optical power signal to feed a photodetector and an RF amplifier, aiming at 5G applications. As a result of experimental measurements, a EVM_{RMS} of approximately 14% was obtained with a modulation order of 16-quadrature amplitude modulation (QAM).

Table 1.1 presents a comparison between this work with the state-of-the-art on PoF system. One may notice that for each application, the fiber type is a critical choice. The DCF and MCF are interesting options due to the possibility of transmission of data and high values of power in the same fiber. However, as a special fiber, it has a high cost and low availability. The SMF is a suitable option to use the infrastructure already installed and transmitting power along with data, although the small core limits the maximum optical power that is possible to transmit. The MMF are also widely used for low-distance communication and have a larger core area than the SMF, allowing to deliver higher optical powers. Nevertheless, is necessary some techniques to transmit high data rates for long distances. The core diameter of the MMF has some variations of size. Although, the larger the core diameter greater the maximum optical power delivered in the PoF system, the 100, 105, or even 200 μm MMF are not conventional fibers. In contrast, the 62.5 μm MMF is a standardized, conventional, and broadly commercialized fiber, having installed infrastructure in communication systems. Therefore, the use of this type of fiber in PoF system becomes very attractive.

One can also note that most of the works have not applied the PoF system to feed a component or device, as in [46] and [49] that only measures the electrical power at the PPC output, or in [34] and [35], which only transmitted the optical power, without any OE conversion. Another potential of this work is the use of the 62.5 μm conventional MMF for the optical power transmission in order to power devices located at the mobile access network.

Table 1.1: *State-of-the-art on PoF system*

Year/ Reference	Powered device	PoF application/ Power transmitted/ HPLD wavelength	Fiber type (core/clad)/ length(m)	Electrical output power (W)	PPC efficiency/ PTE (%)	Wireless communication standard/Reach(m)
2021/ [35]	None	Transmitting simultaneously power and data in a same SMF fiber/ 10 W/1064.8 nm	SMF(8.2/125 μm)/ 1000	-	-	5G NR/ not applicable
2021/ [34]	None	Transmitting simultaneously power and data in a same SMF fiber aiming for IoT applications/ 2 W/1480 nm	SMF(8.2/125 μm)/ 10000	-	-	5G NR/ 0.7
2020/ [46]	None	Transmitting simultaneously power and data in a same DCF fiber/ 150 W/808 nm	DCF(8/125 μm)/ 1000	7.08	24/4.84	IEEE 802.11a/ not applicable
2015/ [49]	None	Transmitting simultaneously power and data in a same DCF fiber/ 4 W/830 nm	DCF(9/105 μm)/ 100	0.4	28.6/10*	IEEE 802.11g/ not applicable
2022/ [50]	None	Transmitting simultaneously power and data in a same MCF fiber/ 60 W/1064.8 nm	MCF(9/150 um)/ 1000	-	-	5G NR/ not applicable
2022/ [37]	RoF module (photodetector and a electrical amplifier)	Feeding a RoF module in a 5G NR network/ 2.2 W/975 nm	MMF(100/140 μm)/ 100	0.516	30/23.5	5G NR/ 10
2018/ [38]	Proximity sensor	Feeding a proximity sensor for hazard environment applications/ 1.5 W/808 nm	MMF(200/500 μm)/ 300	0.36	52/24*	not applicable
2018/ [39]	None	Transmitting simultaneously power and data in a same MMF fiber/ 10 W/1550 nm	MMF(62.5/125 μm)/ 4000	-	-	IEEE standard/ not applicable
2008/ [40]	Short range remote unit (laser, photodector, electrical amplifier)	Feeding a short range remote unit/ 250 mW/834 nm	MMF(62.5/125 μm)/ 300	0.1*	50/40*	IEEE 802.11g/ not applicable
Paper 1	RoF module (photodetector and an electrical amplifier)	Feeding a RoF module, aiming industrial 5G NR communications/ 5 W/808 nm	MMF(62.5/125 μm)/ 100	0.87	23.75/19	5G NR/ not applicable
Paper 3	VLC laser and a RoF module (photodetector and an electrical amplifier)	Feeding a RoF module and VLC laser, aiming indoor 5G NR communications/ 8.1 W/808 nm	MMF(62.5/125 μm)/ 500	1.06	23.75/14	5G NR/ 3

*The presented value was calculated from the corresponding reference.

1.3 Research Contributions

The main contributions of this work are listed below:

- The use of the conventional MMF with 62.5-μm core diameter to transmit 5 W of optical power in a PoF system, aiming to feed a RoF receiver in a 5G NR network applied to an industrial environment.
- An experimental implementation of an optically-powered VLC and RoF-based 5G NR system with dual-access networks utilizing a 62.5 μm conventional MMF capable of feeding two different devices, a RoF module and a VLC red laser, from a remote site, using a unique PPC.
- Application of a PoF system in a 5G network with simultaneous RF and VLC

data links.

1.4 Dissertation Outline

This dissertation is structured in four chapters. Chapter 2 is concerning the technical background of the two main technologies exploited in this work, namely: PoF and VLC. First, it is presented a detailed description of Power over Fiber systems, including its main components. Moreover, the VLC technology concept, features, scenarios and main properties is described. In Chapter 3, the main scientific papers resultant from this work are reported. Finally, the conclusions and future works are addressed in Chapter 4.

Chapter 2

Technical Background

THIS chapter presents a technical background on the PoF and VLC technologies, including the characterization of the main components of the implemented PoF and VLC-based 5G and 6G networks.

2.1 Power-over-Fiber System

2.1.1 High-Power Laser Diode

The HPLD is an optical source based on semiconductor material capable of generating a high level of optical power, on the order of units to tens of watts, and is a very common option to be used in PoF systems [53]. Semiconductor lasers can provide high optical power levels with higher electrical-to-optical (EO) conversion efficiency (above 50%) and smaller sizes, when compared with other laser types, such as the gas laser [54–56]. Moreover, in PoF systems, the HPLD comprises mostly a pigtail in the output. The fiber type of the pigtail needs to match the optical fiber that will be used for the light transmission, which can be connected by splicing or connectors. This is a critical moment, since a mismatch between the core diameter of the fibers, will result in an optical power loss, which can be dangerous for PoF applications.

The operating wavelength of a semiconductor laser is based on the material composition. For instance, inside of an Erbium-doped fiber amplifier (EDFA), there is a pumping laser that operates at 980 nm and is based on Indium Gallium Arsenide (InGaAs). Lasers used in optical communications operate mainly in 1550 nm, and their material is typically the Indium Gallium Arsenide Phosphide (GaInAsP) [57]. In this work, we have used a 12 W- HPLD, model TY80812W01, that operates at 808 nm, with 4 nm of linewidth, and has the Gallium Arsenide (GaAs) as the composition mate-

rial [57]. Figure 2.1 reports the experimental characterization of our HPLD. One may notice the threshold current is about 0.75 A with a voltage level of approximately 4.9 V. From this point onward, the optical power tends toward a linear behavior, accompanied by an increasing EO conversion efficiency.

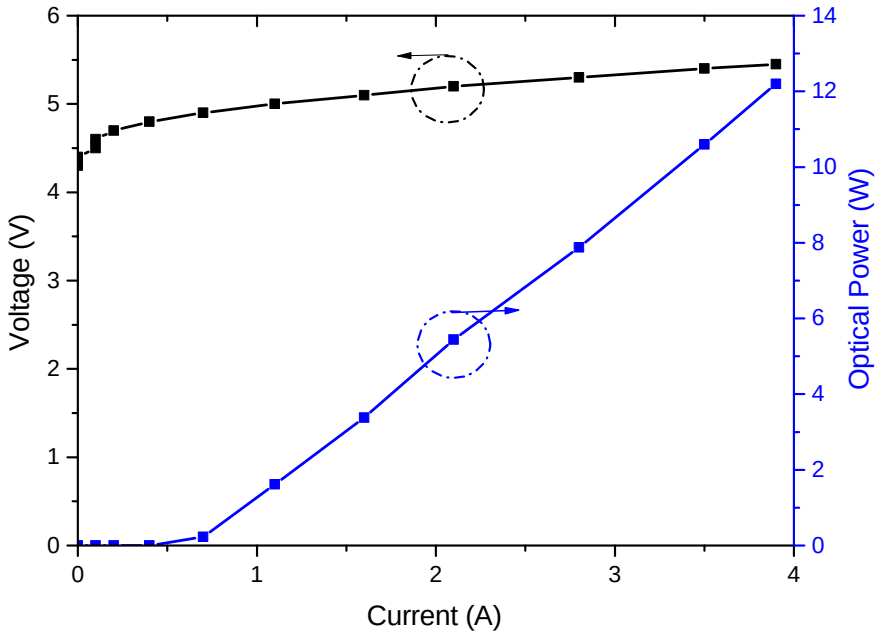

Figure 2.1: *12 W- HPLD output power and voltage as a function of the current.*

Our HPLD has an efficiency of 45%, which indicates the laser needs nearly 2.2 W-electrical power to provide 1 W- optical power at its fiber pigtail. Among the factors that have an impact on the conversion efficiency of the HPLD laser, we can cite the temperature variation. Since the laser is based on semiconductor material, the temperature increase can raise the electric resistivity due to the thermal agitation of the electrons. Consequently, the electric current, and thus the electrical power of the laser, also increases, leading to a reduction in efficiency [58, 59]. Temperature can also change the wavelength of the laser, approximately 0.3 nm/°C for our laser. In this context, we have configured a thermoelectric cooler (TEC), model TED200C, based on the Peltier effect and a temperature controller, in order to cool the HPLD and guarantee a stable efficiency. A photograph of our HPLD setup with the TEC may be seen in Figure 2.2.

2.1.2 Optical Fiber

The optical fiber is the main component for making the use of PoF technique feasible, due to its inherent characteristics, such as electromagnetic interference immunity, galvanic isolation between source and load, noncorrosive material, lightweight, and lower attenuation when compared to copper wires [60]. In PoF systems, the attenua-

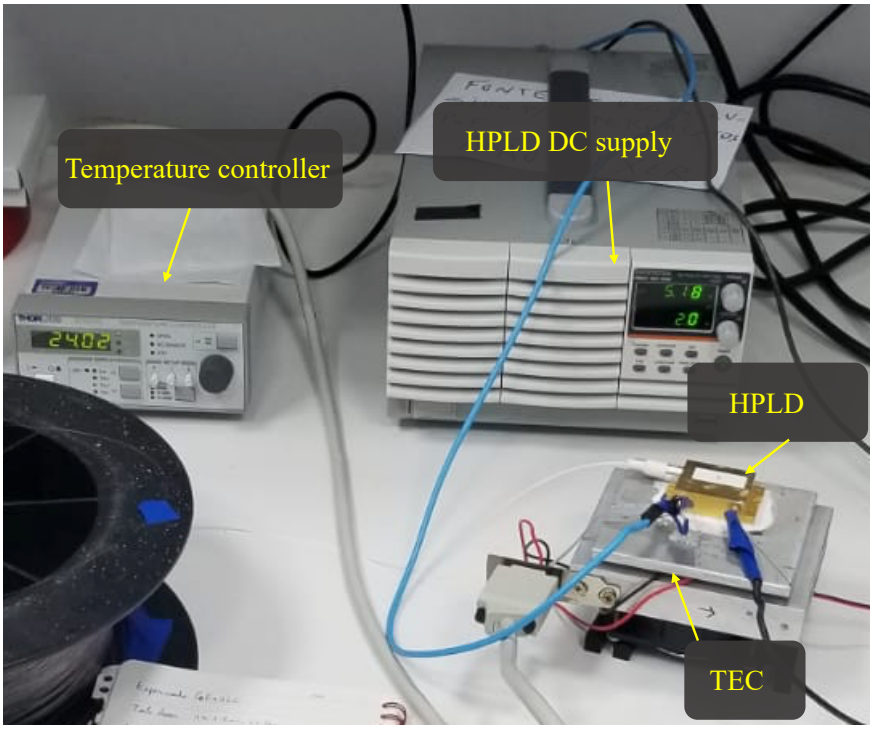

Figure 2.2: *Photograph of the 12 W- HPLD setup.*

tion of the optical fiber must be always verified before inserting a fiber spool into the system. The attenuation of a signal propagating in a certain material depends on the frequency of wavelength of this signal. Typically, a silica-based fiber has a minimum attenuation of around 0.25 dB/km nearly in the 1550 nm band. On the other hand, the HPLD operates between 800-1000 nm, and the optical fiber attenuation has a higher value in this window, approximately 2 to 3 dB/km [61]. In this context, to power a component that needs 5 W electrical power for proper operation, an HPLD would need to launch 10 W optical power into the fiber of 1 km link length, considering 3 dB/km of fiber attenuation, 100% of OE conversion efficiency, and not considering the connectors, adaptors, and splice losses.

Another important parameter regarding optical fibers is the threshold power that is allowed to transmit in a fiber without damaging it. From empirical analysis, it is possible to consider that silica-based optical fibers have a maximum power density of one to several MW/cm^2 [38, 62]. The threshold power (P_{th}) that can be launched in an optical fiber can be determined by [38]

$$P_{\text{th}} = A_{\text{eff}} I_{\text{th}} = \pi \left(\frac{d_{\text{mfd}}}{2} \right)^2 I_{\text{th}} \tag{2.1}$$

where A_{eff} is the effective cross-sectional area of the propagating wave, I_{th} is the threshold power density, and d_{mfd} is the fiber mode field diameter (MFD). Analyz-

ing Equation 2.1, it can be noticed that the larger the core, the greater the maximum power allowed to be transmitted in an optical fiber without any damage. For example, considering 2.5 MW/cm^2 of maximum power density [38], the threshold power in a 9 μm-SMF for 1550 nm, and a 62.5 μm MMF for 808 nm, are 1.38 and 32.83 W, respectively. For these calculations, the effective area of the MMF was obtained by [63]

$$A_{\text{eff}} = \pi w^2 = \pi[r(0.65 + 1.659V^{-1.5} + 2.879V^{-6})]^2 \tag{2.2}$$

where w is the core effective radius, r is the fiber core radius, and V is the V number of the fiber, which can be determined by [63]

$$V = \frac{2\pi r NA}{\lambda} \tag{2.3}$$

where NA is the fiber numerical aperture and λ is the wavelength.

Due to the high optical power level launched into the optical fiber, some nonlinear effects must be taken into consideration. Among them, we can highlight the stimulated Raman scattering (SRS) and stimulated Brillouin scattering (SBS) [64]. SRS is the interaction between incident photons from a light source and the molecules of the optical fiber. During this process, molecules absorb energy from the photons, resulting in a decrease in the photon energy and, consequently, an increase in wavelength, making them longer than when initially incident into the optical fiber [61]. Therefore, the threshold power to the SRS appears (P_{SRS}) is given by [62]

$$P_{\text{SRS}} = \frac{16A_{\text{eff}}}{g_{\text{R}} L_{\text{eff}}} \tag{2.4}$$

where g_{R} is the Raman gain coefficient, around 5×10^{-14} for non-polarized light, and L_{eff} is the effective fiber length, which can be obtained by [62]

$$L_{\text{eff}} = \frac{1 - e^{-\alpha L}}{\alpha} \tag{2.5}$$

where α is the fiber attenuation and L is the fiber length.

In contrast, the SBS occurs when high optical power levels generate an acoustic wave in the fiber, leading to fluctuations in the refractive index. These variations cause photons to scatter back towards the light source with a different wavelength, resulting in a subsequent reduction in signal power [61]. The SBS threshold power (P_{SBS}) is defined as [61].

$$P_{\text{SBS}} = \frac{21 A_{\text{eff}} b}{g_{\text{b}} L_{\text{eff}}} \left(1 + \frac{\Delta v_{\text{source}}}{\Delta v_{\text{B}}}\right) \tag{2.6}$$

where b is the polarization factor that lies between 1 and 2, g_{b} is the Brillouin gain coefficient which is approximately 4×10^{-11}, Δv_{source} is the optical source linewidth, and Δv_{b} is the linewidth of the scattered optical signal due to the Brillouin effect (35 MHz) [61, 62].

To evaluate the threshold value of SBS and SRS, we performed a simulation using Equations 2.4 and 2.6, considering the 12-W HPLD and the 62.5 μm core diameter MMF. Figure 2.3 presents the threshold of both effects as a function of the link length. One may notice that the threshold for SBS is nearly 200 times higher than that for SRS, at least up to a link length of 10 km. For distances greater than 3 km, SBS and SRS will occur around 50 and 0.25 KW of optical power, respectively. Since our HPLD has a maximum power of 12 W, this level of power is insufficient for these effects to occur and impact the PoF functionality.

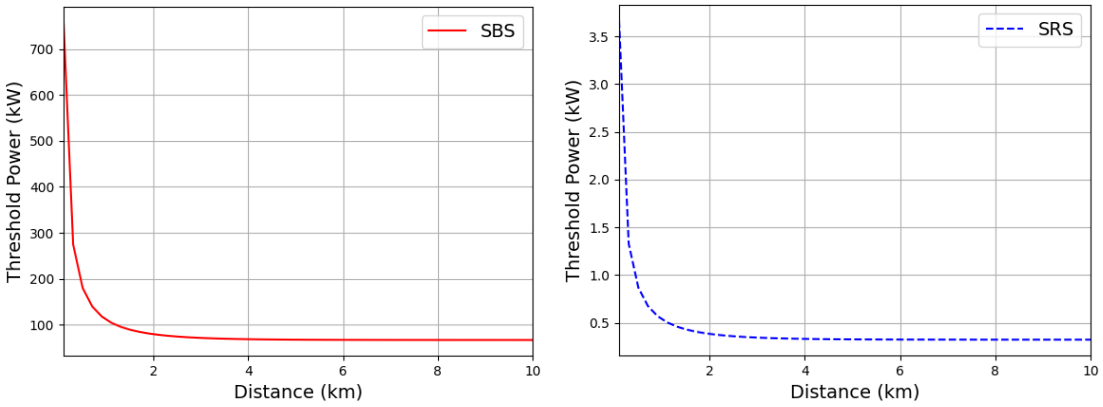

(a) *SBS thresholds as a function of the link distance.*

(b) *SRS thresholds as a function of the link distance.*

Figure 2.3: *Brillouin and Raman thresholds as a function of the link distance for our 12 W-HPLD and 62.5 μm fiber.*

Regarding the experimental characterizations, we used the conventional MMF with 62.5 μm of core diameter and different link lengths (from 100 up to 1000 m). In addition, we utilized the optical power transmission efficiency (OPTE), which is a metric that indicates the ratio between the optical power collected from the fiber output and the optical power in the HPLD output [65]. This metric is important to evaluate the total optical power loss, which includes the fiber attenuation and the loss in connectors, adaptors, and splice. Consequently, through this analysis, the feasibility of each fiber link length implementation was evaluated. Table 2.1 reports the OPTE values of 100, 200, 500, and 1000 m of fiber link lengths. From these results, we have chosen the 500 m link, since it is the maximum distance we can achieve due to the maximum

power of the HPLD and the required power of the target load. The load characteristics will be further discussed. The OPTE curve for 500 m link length as a function of the optical input power might be seen in Figure 2.4. One may notice the maximum optical output power is approximately 7 W, which would be entering the PPC, with approximately 60% of OPTE. Another important observation is about the lower OPTE values for input power up to 3 W. Initially, this behavior was attributed to the low efficiency of the HPLD at lower levels of optical power. However, since the OPTE does not account for the HPLD efficiency, this analysis was discarded. Currently, this phenomenon is under investigation to discover the reason for these low OPTE values observed for optical powers below 4 W.

Table 2.1: *OPTE as a function of the link length.*

Link length (m)	OPTE
100	84.89%
200	80.62%
500	58.67%
1000	41.95%

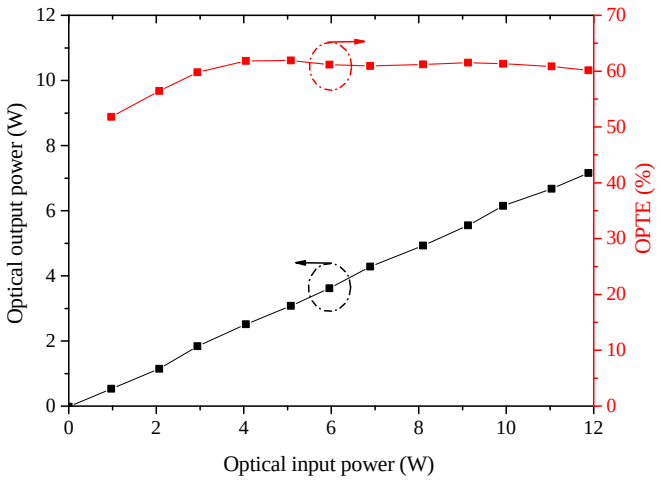

Figure 2.4: *Optical power transmission efficiency for 500 m link length.*

2.1.3 Photovoltaic Power Converter

The PPC is responsible for performing the OE conversion and is a critical component in PoF systems. The PPC comprises solar cells, similar to the solar panels, which receive energy from photons to generate free electrons, according to the photovoltaic effect. To maximize the efficiency, the PPC must be compact to match the beam diameter output of the fiber end-face [66]. Furthermore, for comparison, the PPC demonstrates notably higher conversion efficiency than conventional solar pan-

els. This may be attributed to it is design, optimized for a specific wavelength range of laser operation, unlike solar panels that receive broadband solar radiation [67].

The main parameters of a PPC when inserted in a PoF system are the conversion efficiency, wavelength range, and maximum input power. These parameters are associated mostly with its composition material. For example, with a range of efficiency from 15 to 60%, the most common materials are Silicon (Si), GaAs, InGaAs, and Gallium Antimonide (GaSb) [68, 69]. Table 2.2 reports two commercial PPCs with their respective material, maximum input power, optimum wavelength, and efficiency [33]. One may notice that, although GaAs has a higher efficiency than Si, the Si-based PPC enables the achievement of an electrical output power of approximately 2.4 W, whereas the GaAs-based PPC provides around 0.825 W.

Table 2.2: *Parameters of two available commercial PPCs [33].*

Device (material)	Maximum input power (W)	Conversion efficiency (%)	Optimum wavelength (nm)
Si	10	24	900-980
GaAs	1.5	55	800-850

In this work, it was utilized a Si-based PPC, model YCH-H6424-15-SM-B, which supports up to 20 W. A photograph of the PPC may be observed in Figure 2.5. A DC/DC converter, model DDH1800, was inserted at the PPC output to adjust the voltage level for the load. An evaluation of conversion efficiency and electric output power was experimentally performed, as is reported in Figure 2.6a. The maximum obtained electrical power was around 5 W for an optical input power of 20 W and 980 nm,

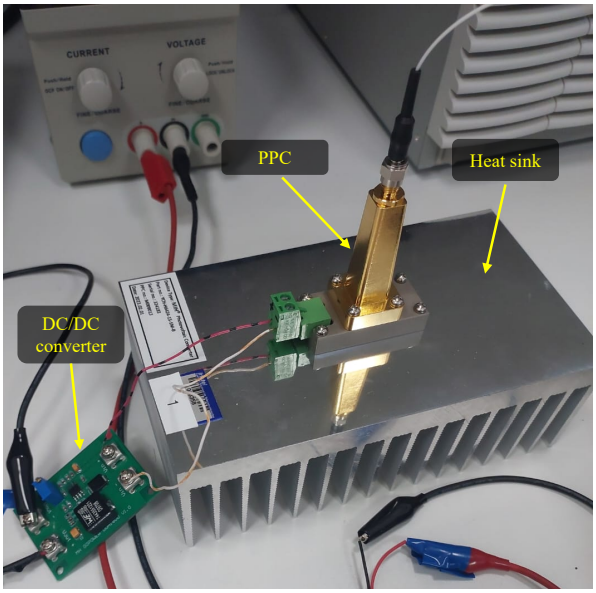

Figure 2.5: *Photograph of the 20 W-PPC with a DC/DC converter coupled at the output.*

achieving nearly 25% conversion efficiency. Another experimental characterization involved obtaining the IV-curve, which illustrates the relationship between voltage and current levels at the PPC output. This IV-curve is presented in Figure 2.6b. One may notice that the PPC provides a maximum current level of approximately 0.3 A, for an optical input power of 20 W. When the circuit is open, the voltage level is nearly 22 V. It is important to emphasize that for each optical input power, there is an optimum load to achieve the best conversion efficiency, i.e., the maximum power point (MPP) [70]. In order to control the variation in the resistive load, it was used a system DC electronic load, model 6063B, from HP.

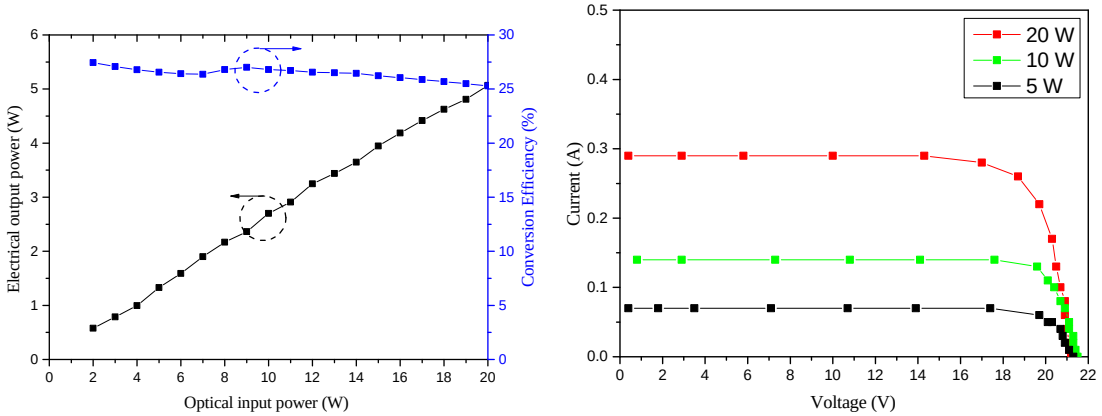

(a) *Conversion efficiency and electrical output power of the PPC as a function of the 980 nm-optical input power.*

(b) *PPC characterizations of current as a function of terminal voltage level for 5, 10, and 20 W optical input powers.*

Figure 2.6: *20 W-PPC characterizations.*

Since our HPLD provides optical power at 808 nm, out of the optimum wavelength range of silicon, the PPC was not performed at its best efficiency. Therefore, an experimental comparison between two HPLDs with different operating wavelengths, 980 nm and 808 nm, was carried out to evaluate the PPC efficiency drop. Table 2.3 reports the conversion efficiency for 2, 5, and 10 W optical power for both HPLDs. As expected, the PPC has a reduction in the efficiency at 808 nm with a maximum drop of 10.5% for 2W optical power.

Another important metric to evaluate the performance of a PoF system is the PTE,

Table 2.3: *Comparison of PPC conversion efficiency as a function of wavelength*

-	Laser wavelength	
Optical input power (W)	980 nm	808 nm
2	29%	18.5%
5	26.6%	22.1%
10	27%	19.1%

which describes the ratio between the electrical output power obtained from the PPC and the optical power provided by the HPLD [66]. An experimental test, similar to the OPTE, was carried out to obtain the PTE values for different link lengths, as is presented in Table 2.4. Due to the required electrical power at the PPC output, the 500 m link was utilized, and, the PTE and the electrical output power curves as a function of the optical input power were obtained, as is reported in Figure 2.7. It can be observed the maximum electrical power is approximately 1.75 W for 12 W optical power, with a PTE mean value of nearly 13.75%. Moreover, as expected, the same behavior of OPTE values for optical input power below 4 W is observed in the PTE curve, since the electrical output power depends on the optical power at the fiber end.

Table 2.4: *PTE as a function of the link length*

Link length (m)	PTE
100	19.11%
200	18.57%
500	13.75%
1000	8.93%

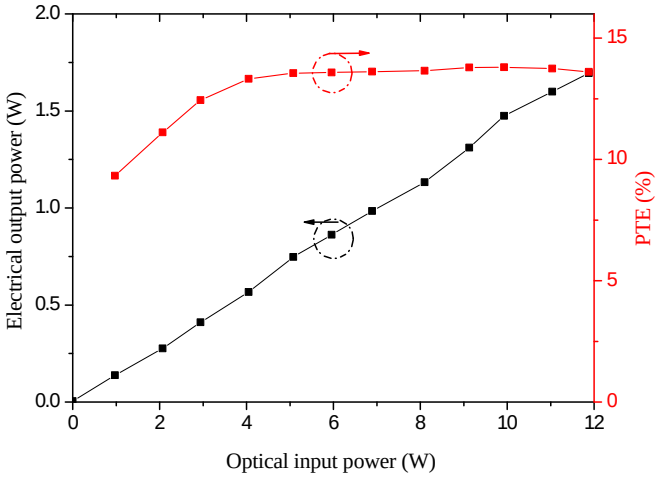

Figure 2.7: *Power transmission efficiency for 500 m link length.*

2.2 Visible Light Communication System

The VLC operates in the spectrum range from 400 to 700 nm, basically comprising a transmitter, light-emitting diode (LED) or light amplification by stimulated emission of radiation (laser), and a photodetector as a receiver [71]. Lasers offers a larger bandwidth and a higher spectral and spatial coherence than LEDs, enabling it to reach longer distances at higher data rates [72]. However, LEDs enables coverage of a broader area and might be applied in a multipoint topology [73]. Figure 2.8 presents

an application scenario for the VLC technology, where LED lamps are used not only to illuminate the room but also to provide communication.

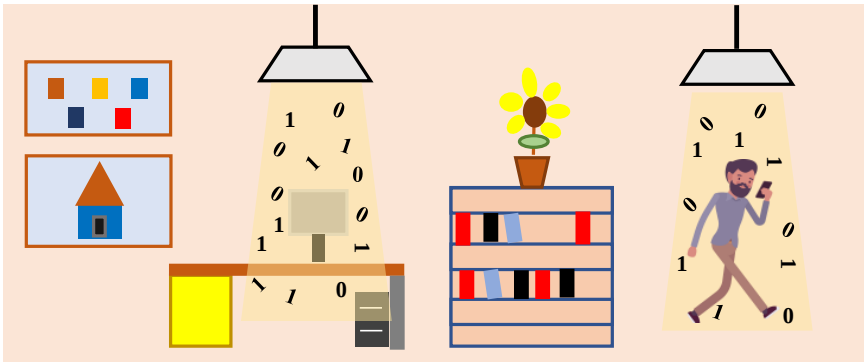

Figure 2.8: *Application scenario of VLC technology.*

In this work, the transmitter of our VLC setup was composed of a red laser-diode-mount device, which has a bias tee (BT) and a thermoelectric actuator. In addition, a TEC set at 25ºC was used to guarantee stable optical power, and, a 20 mA electric current for the laser operation was supplied by the PoF system. On the receiver side, an achromatic lens was used to focal the beam into the photodetector input. The schematic setup might be observed in Figure 2.9.

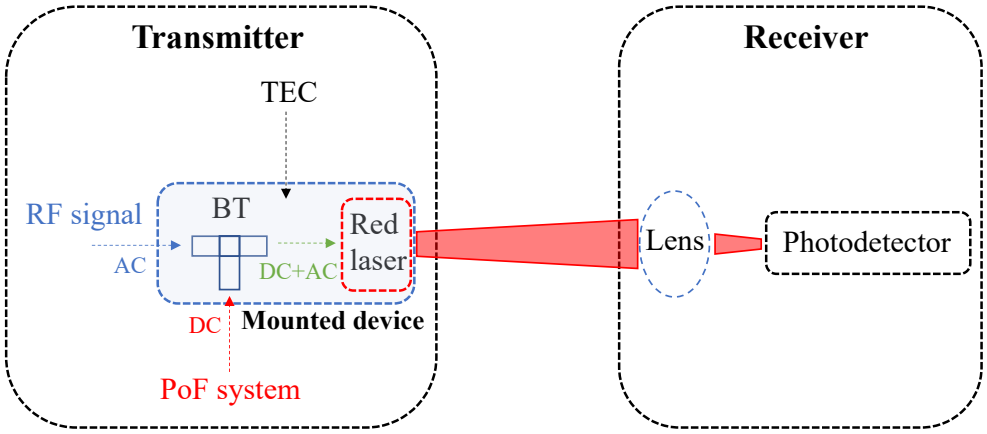

Figure 2.9: *Schematic setup of the implemented VLC system.*

The VLC with only one color was used as proof of concept in using a PoF system to feed an OWC as an access network. Moreover, the reason for using the red laser was based on the PIN photodetector (model EOT 2030) responsivity and the frequency response of the lasers (red, green and blue). According to the photodetector responsivity, presented in Figure 2.10, there is a peak of 0.5 A/W at approximately 800 nm. Consequently, the red laser, which operates at 650 nm, has a better response than the green (520 nm) and blue (450 nm) lasers. Regarding the frequency response of the lasers, a frequency sweep from 10 MHz to 1 GHz was configured, in order to analyze the laser behavior in this frequency range. Figure 2.11 reports the three characterizations, where

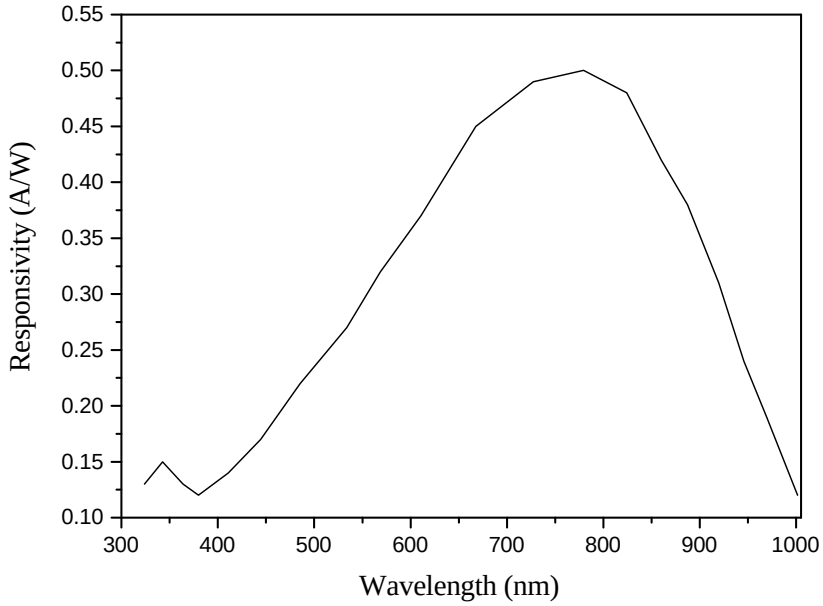

Figure 2.10: *EOT 2030-photodetector responsivity.*

the red laser magnitude predominates for almost all the frequency range. The choice of the signal central frequency to modulate the VLC carrier was also based on the 5G NR frequency range 1 (FR1), which starts from 410 MHz, according to the 3rd Generation Partnership Project (3GPP) Release 18 [74]. Therefore, different central frequencies from 410 to 650 MHz were evaluated, and through experimental tests, the frequency of 650 MHz obtained the best performance and it was chosen for the experiments.

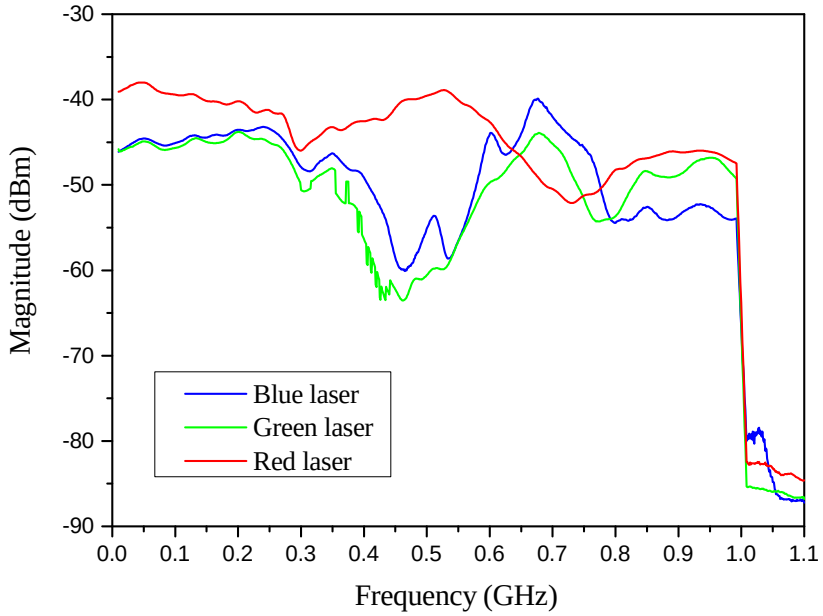

Figure 2.11: *Frequency response of the red, green, and blue laser.*

2.3 Power-over-Fiber System Applied to 5G/6G Networks

This Section reports the highlights of the two implemented PoF systems applied to 5G/6G networks. The methodology and main results are presented in Paper 1 and Paper 2 from Chapter 3.

2.3.1 Paper 1: "PoF System Using Standard 62.5-micron Multimode Fiber for 5G NR Industrial Applications"

In Paper 1 we have implemented an optically-powered RoF-based 5G NR system, aiming to use PoF technique in an industrial environment. A photograph of the PoF and RoF setups is presented in Figure 2.12.

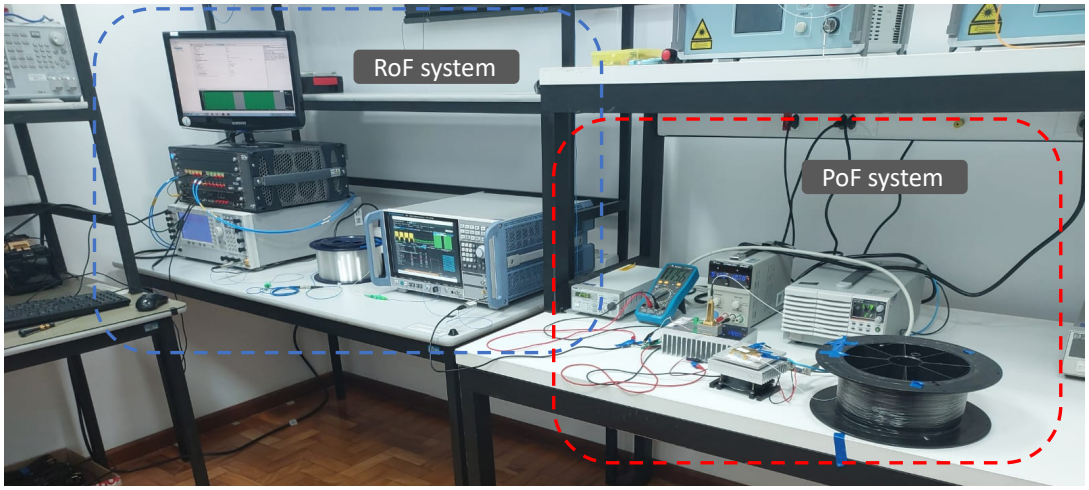

Figure 2.12: *Photograph of the optically-powered RoF-based 5G NR system.*

The highlights of Paper 1 are listed below:

- The PoF system comprised the following components: 12-W HPLD with TEC; 100 m 62.5 μm MMF; 20 W PPC; and finally a DC/DC converter.
- 5W optical power was transmitted, aiming to feed a RoF receiver in a RoF-based 5G NR network.

2.3.2 Paper 2: "Optically-Powered Hybrid VLC/FiWi System Towards 6G"

Paper 2 represents an evolution from the previous one, both in the communication and in the PoF systems. A 5G network envisaged for indoor scenarios, was designed using the RoF technique for the optical fronthaul, and two systems were simultaneously implemented for a dual access network: an RF wireless and a VLC link. The

PoF system was configured to feed simultaneously two components at the remote site, the RoF receiver and the VLC laser, using a unique PPC. The full setup might be observed in Figure 2.13.

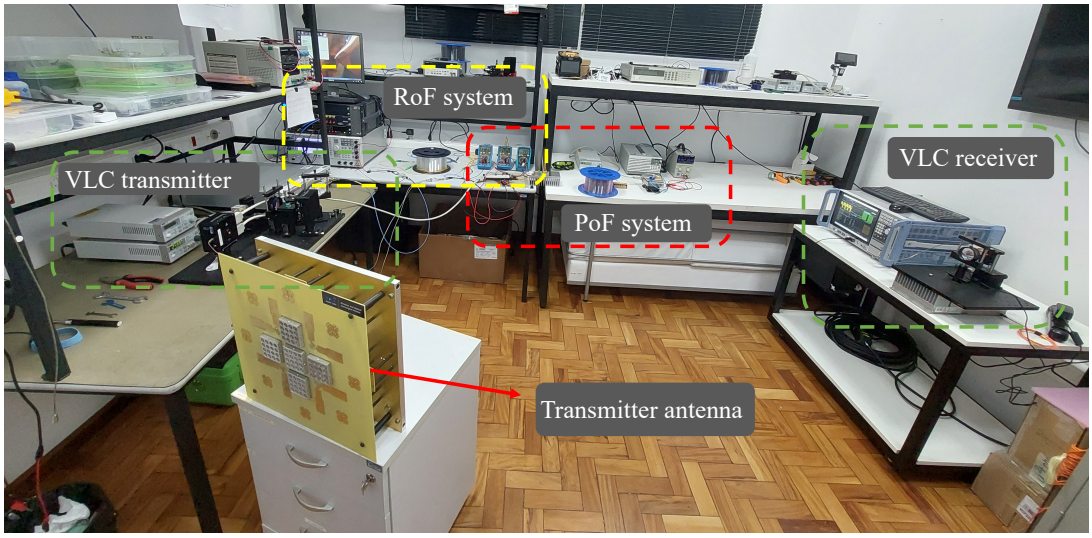

(a) *Implemented setup of the PoF- 5G NR system with dual access.*

(b) *Receiver setup.*

Figure 2.13: *Photograph of the optically-powered hybrid VLC/FiWi system towards 6G.*

The highlights of Paper 2 are listed below:

- The implemented PoF system comprised the same HPLD from the previous work, but in this case, it was set to transmit 8.1 W throughout 500 m of 62.5 μm MMF link. In the output of the 20 W PPC, two DC/DC converters were set to

regulate the voltage level for each load.

- The RoF receiver and VLC red laser were simultaneously fed using a unique PPC.
- Two electrical generators were used to generate the VLC and RF wireless signals.
- Two power splitters were used to combine and divide both data signals.
- The 5G NR access networks were composed of a 3m- VLC link using a red laser, and also a 3m- RF wireless link.

Chapter 3

Summary of Original Work

This Dissertation is based on a set of papers published or submitted for publication in peer-reviewed journals and conference proceedings. Those papers report the main results of the implementations of PoF systems for optically feeding 5G and 6G networks. The articles are reproduced in this Chapter, followed by complementary discussion on each of them.

Paper 1: PoF System Using Standard 62.5-micron Multimode Fiber for 5G NR Industrial Applications

Felipe Batista Faro Pinto, Letícia Carneiro de Souza, Tomás Powell Villena Andrade, Eduardo Saia Lima, Luis Gustavo da Silva, Francisco Martins Portelinha Junior, Evandro Lee Anderson, Rodnei Carçola and Arismar Cerqueira Sodré Junior. "*PoF System Using Standard 62.5-micron Multimode Fiber for 5G NR Industrial Applications*", accepted in *20th SBMO/IEEE MTT-S International Microwave and Optoelectronics Conference (IMOC 2023)*. **Publisher:** IEEE

PoF System Using Standard 62.5-micron Multimode Fiber for 5G NR Industrial Applications

Felipe Batista Faro Pinto, Letícia Carneiro Souza, Tomás Powell Villena Andrade and Arismar Cerqueira S. Jr.
WOCA Laboratory, National Institute of Telecommunications (Inatel)
Santa Rita do Sapucaí-MG, Brazil
felipe.faro@mtel.inatel.br

Eduardo Saia
5G Innovation Office, VS Telecom
São Paulo, SP
eduardo.lima@vstelecom.com.br

Luis Da Silva, Francisco Portelinha
Inatel Competence Center (ICC)
National Institute of Telecommunications (Inatel)
franciscoportelinha@inatel.br

Evandro Lee A. and Rodnei Carçola
MPTcable
Indaiatuba, SP
evandro.souza@mptcable.com.br

***Abstract*—This paper presents an experimental implementation of a radio-over-fiber (RoF)-based 5G new radio (NR) system and power-over-fiber (PoF) technique for industrial environments. The generated 3.5-GHz 5G NR signal is transmitted throughout a 20-km single-mode optical fiber (SMF) link. Regarding the PoF system, a 5-W optical power is transmitted by means of a 100-m standard multimode optical fiber (MMF) link. A photovoltaic power converter (PPC) and a DC/DC converter are employed to convert the power from the optical to the electrical domain and adjust the voltage level, respectively, aiming to power an RoF module. As a result, the PoF system power transmission efficiency (PTE) is analyzed, reaching a mean value of around 19%, and root mean square error vector magnitude (EVM_{RMS}) performance investigation is conducted to evaluate the 5G transmission. A throughput of 600 Mbps is achieved with 100-MHz bandwidth and without performance degradation when compared to the conventionally powered RoF system, demonstrating the applicability and potential of the PoF technique for 5G NR-based industrial communications.**

***Index Terms*—5G NR, Power-over-Fiber, Standard MMF.**

I. Introduction

The fifth generation (5G) of mobile networks, standardized as new radio (NR), has been implemented over three main application scenarios: enhanced mobile broadband communication (eMBB); massive machine-type communication (mMTC); ultra-reliable low-latency communications (URLLC) [1]. The mMTC scenario, designed for offering low latency and supporting a large number of connected devices and machines, has become a key factor to Industry 4.0 [2]. One of the main challenges in industrial communications is the harsh environment, which is characterized by substantial electromagnetic interference. Therefore, the use of copper wires to supply electrical power to devices could not be suitable on the factory floor [3]. In this context, power-over-fiber (PoF) systems have been showing a huge potential to overcome this issue. The PoF technique consists in transmitting high optical power by means of an optical fiber, in order to power devices in remote locations. The advantages of optical fibers, such as electromagnetic interference immunity, galvanic isolation, lightweight, and lower attenuation compared to copper wires, make the PoF technique attractive for harsh areas in industrial applications [4]. Fig. 1 presents the PoF and a 5G NR transmission in an industrial environment. This scenario is proposed over the centralized-radio access network (C-RAN) architecture, which consists of concentrating all the signal processing in a central office, reducing the power consumption at the receiver side. Moreover, for the 5G NR system, the radio-over-fiber (RoF) technique was employed to perform the data transmission through an optical fiber link.

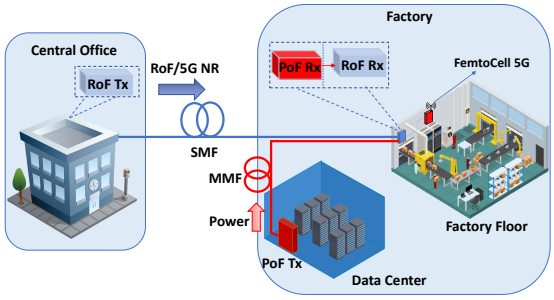

Fig. 1. 5G NR transmission and PoF system in an industrial environment.

The PoF system typically employs three main components: a high-power laser diode (HPLD); an optical fiber; and a photovoltaic power converter (PPC). Several works have investigated the PoF system in different scenarios, using multimode optical fiber (MMF). For instance, the authors in [5] presented a PoF system using a 100-m MMF with a 100-μm core diameter, transmitting 5 W of optical power, aiming at Industrial Internet of Things (IIoT) applications. In [6], the authors demonstrated an RoF and PoF simultaneous transmission in a single standard MMF with 62.5 μm core size. By using the center-launching (CL) and offset-launching (OL) techniques, the dispersion and feed light crosstalk were effectively mitigated in the MMF. Consequently, 10 W of optical power could be co-transmitted with an RoF signal over a 4-km MMF link. Cardona *et. al*, transmitted 1.75 W

979-8-3503-2067-1/23/$31.00 ©2023 IEEE

of optical power over 100 m of an MMF with 200-μm core diameter, in order to supply low-power remote radio heads (RRH) in 5G networks with sleep modes [7]. A PoF system transmitting 1.5-W optical power through a 300-m MMF with 200-μm core diameter was reported in [8], aiming to supply smart remote nodes.

This paper main contribution is the use of the standard MMF with 62.5-μm core diameter to transmit 5 W of optical power in a PoF system, aiming to feed the RoF Rx in a 5G NR network. To the best of our knowledge, we have employed a standard MMF in a PoF-based 5G NR system applied to industrial applications for the first time in the literature. The manuscript is structured in four sections. Section II reports the experimental implementation, describing all equipment used, whereas Section III presents the obtained results from the performance investigation of PoF and RoF systems. Finally, in Section IV the final conclusions are presented.

II. PoF- and RoF-based 5G NR System

In order to analyze and validate the PoF and RoF-based 5G NR system, an experimental setup was assembled. Fig. 2 presents the block diagram of the setup and all the equipment used in the experiment. Regarding the 5G NR waveform generation, an arbitrary waveform generator (AWG), model M8190A, from Keysight, was used. The generated baseband signal was transmitted to a vector signal generator, model E8267D PSG, also from Keysight, to upconvert the 5G NR signal frequency to 3.5 GHz. The RF signal was injected into the RoF Tx module, model A13-Z101-D55-AS-SL, from Optical Zonu Corporation, which has an electric amplifier (EA) and a laser diode (LD). An 4-dBm optical carrier, centered at 1550.06 nm, is generated by direct modulation and transmitted through a 20-km single-mode optical fiber (SMF) link. In order to convert the signal from the optical to the electric domain an RoF Rx module was used, model A23-Z101-00AS-S, also from Optical Zonu Corporation, which is composed of a photodetector (PD) and an EA. Consequently, a vector signal analyzer (VSA), model FSW, from Rohde & Schwarz, was configured to demodulate the 5G NR signal.

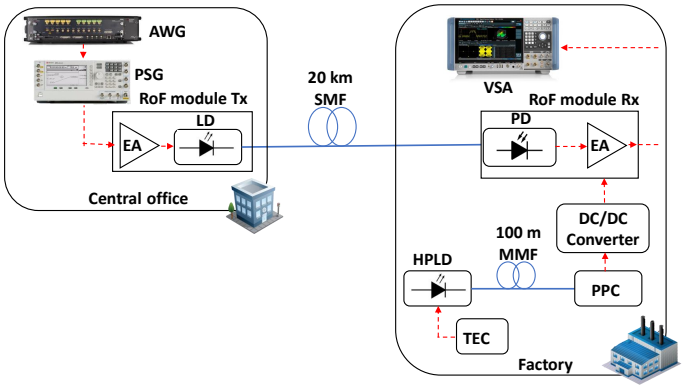

Fig. 2. Block diagram of the experimental setup.

Regarding the PoF system, a 12-W HPLD, model TY80812W01, operating at 808 nm was set to transmit 5 W over the 62.5-μm core diameter MMF. The 100-m MMF link was coupled to the HPLD optical fiber output by means of splicing since both fibers have the same core diameter. The total PoF link attenuation was approximately 0.9 dB, which includes the splice and MMF loss at 808 nm. We have used a temperature controller (TEC) model TED200C, from Thorlabs, to control the laser temperature and maintain the system stability during all the experiments. The optical link output was connected to a 20 W PPC, model YCH-H6424-15-SM-B, from MH Go Power. Sequentially, a DC/DC converter was employed at the PPC output to adjust the voltage level to 5 V, which is required by the RoF Rx module.

III. Experimental Results

According to the datasheet [9], the RoF Rx module operates at a maximum electrical current supply of 160 mA. At 5-W HPLD output optical power, the PPC, along with the DC/DC converter, was capable of providing around 117 mA of electric current and a voltage level of 5.15 V for the RoF module connected as a load, which is sufficient to feed the RoF Rx. Additionally, a multimeter was used to monitor the electric current value during the experiment, as can be seen in the experimental setup, reported in Fig. 3.

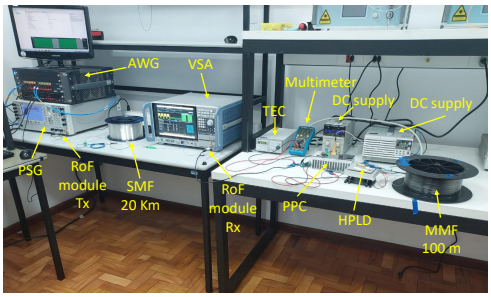

Fig. 3. Photograph of the experimental setup.

In order to analyze the PoF system efficiency, the optical power provided by the HPLD was varied from 1 W up to 12 W. The delivered electric current and the voltage level were measured for each optimal load by using a system DC electronic load, model 6063B, from Hewlett Packard (HP). Consequently, the electrical power was calculated to estimate the power transmission efficiency (PTE) of the PoF system, which describes the relation between the electrical power in the PPC output and the input optical power of the system. This parameter is illustrated in Fig. 4. As it might be observed in Fig. 4, the PPC output electric power increases linearly with the HPLD input optical power. The system losses comprise optical fiber attenuation, fusion splicing loss, and PPC conversion efficiency (around 23.75% at 808 nm). Moreover, it can be observed that the PTE value of 19% is practically constant for all measurements. This stability can be associated with the temperature control in the HPLD, and also with a large heat sink coupled in the PPC.

The performance metric used to evaluate the RoF 5G NR system was the root mean square error vector magnitude (EVM_{RMS}). In summary, the EVM_{RMS} indicates the mean

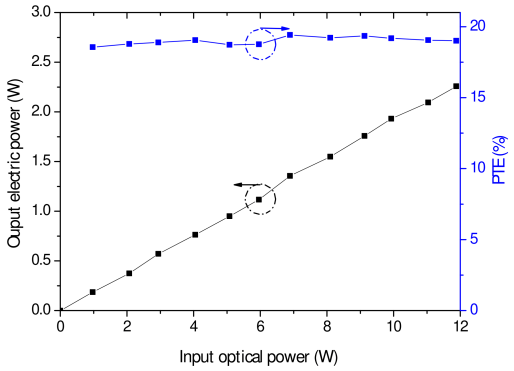

Fig. 4. Output electric power and PTE as a function of the input optical power.

value of the difference between where is the received symbol and its ideal location. Fig. 5 presents the EVM_{RMS} as a function of the RF input power into the RoF Tx module and also the EVM_{RMS} limits standardized by the 3rd Generation Partnership Project (3GPP) Release 18 for each modulation order [10]. In the AWG, the 5G NR signal was configured with 50-MHz bandwidth and the modulation order was set to quadrature phase shift keying (QPSK), 16 quadrature amplitude modulation (QAM), 64 QAM, and 256 QAM. One can note that, for RF power values higher than approximately -33 dBm, all the analyzed modulation orders present EVM_{RMS} below the 3GPP limits. Moreover, it is possible to observe that the lowest EVM_{RMS} is achieved at -17-dBm RF power, i.e. best operation point, for all the modulation orders. On the other hand, for RF power values higher than -14 dBm, the EVM_{RMS} increases due to the RoF Tx EA saturation. The EA operates in the nonlinear region, generating harmonics and intermodulation products.

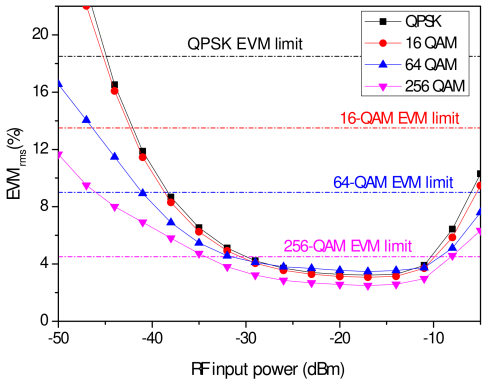

Fig. 5. EVM_{RMS} as a function of the RF power.

We have performed a second PoF characterization to evaluate the RoF performance dependence on the power supply, i.e., PoF-based power supply and using a conventional DC source for powering the RoF Rx module. For this purpose, a 100-MHz bandwidth 5G NR signal with 64 QAM modulation was configured, reaching the maximum throughput of 600 Mbps. Fig. 6 presents the comparison of EVM_{RMS} as a function of RF power in the RoF Tx input, for both scenarios. One can observe a high level of similarity between both approaches, validating the proposed PoF system.

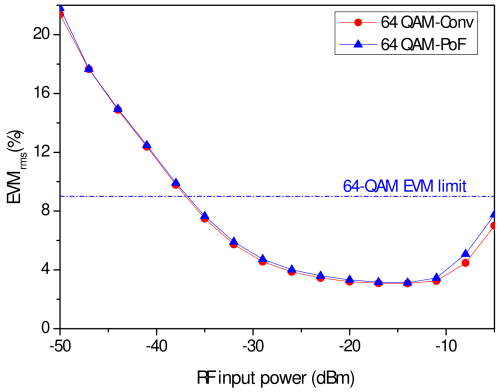

Fig. 6. EVM_{RMS} comparison between PoF system and conventional supply.

IV. Conclusions

The PoF technique was successfully implemented to power an RoF Rx module in a 5G NR system. In this context, 5 W of optical power was transmitted over a 100-m standard MMF link to a PPC, reaching around 19% of PTE. An EVM_{RMS} performance analysis demonstrated the feasibility of the proposed 5G NR system for a 50-MHz bandwidth signal with different modulation orders. Finally, a comparison between the PoF and the conventionally powered RoF system, which reached 600-Mbps throughput, demonstrated that the PoF technique is suitable to power RoF-based 5G NR systems for industrial applications.

Acknowledgment

This work was partially supported by RNP, with resources from MCTIC, Grant No. 01245.020548/2021-07, under the Brazil 6G project of the Radiocommunication Reference Center of the Inatel, Brazil, and by Huawei, under the project Advanced Academic Education in Telecommunications Networks and Systems, contract No PPA6001BRA23032110257684. The authors also thank the financial support from CNPq, CAPES, FINEP, FAPEMIG, FAPESP, and MPTcable.

References

[1] H. R. D. Filgueiras *et al.*, "Wireless and optical convergent access technologies toward 6G," *IEEE Access*, vol. 11, pp. 9232–9259, 2023.
[2] M. Kottkamp *et al.*, *5G New Radio: Fundamentals, procedures, testing aspects*. Rohde & Schwarz GmbH & Company KG, 2019.
[3] C. Budelmann, "Opto-electronic sensor network powered over fiber for harsh industrial applications," *IEEE Transactions on Industrial Electronics*, vol. 65, no. 2, pp. 1170–1177, 2017.
[4] Werthen *et al.*, "Power over fiber: a review of replacing copper by fiber in critical applications," *Optical Technologies for Arming, Safing, Fuzing, and Firing*, vol. 5871, pp. 85–90, 2005.
[5] L. C. Souza *et al.*, "Optically-powered wireless sensor nodes towards industrial Internet of Things," *Sensors*, vol. 22, no. 1, p. 57, 2021.
[6] H. Kuboki and M. Matsuura, "Optically powered radio-over-fiber system based on center-and offset-launching techniques using a conventional multimode fiber," *Optics Letters*, vol. 43, no. 5, pp. 1067–1070, 2018.
[7] J. D. L. Cardona *et al.*, "Optically feeding 1.75 W with 100 m MMF in efficient C-RAN front-hauls with sleep modes," *Journal of Lightwave Technology*, vol. 39, no. 24, pp. 7948–7955, 2021.
[8] J. D. López-Cardona, D. S. Montero, and C. Vázquez, "Smart remote nodes fed by power over fiber in Internet of Things applications," *IEEE Sensors Journal*, vol. 19, no. 17, pp. 7328–7334, 2019.
[9] "RoF Transmitter and Receiver OZ10x OEM," *Optical Zonu*, 2021.
[10] "3GPP TS 38.141-1. Base Station (BS) conformance testing, Part 1: Conducted conformance testing, Release 18." 2023.

3.1 Complementary discussion on the Paper 1

It has been noted a performance degradation (EVM_{RMS} increase) for RF output levels higher than -8 dBm at the RoF tx module input. Such behavior could be observed by analyzing Fig. 5 from paper 1 and it can be also inferred from Figure 3.1 below, which shows an increase in the noise floor when the RF power is increased from -16 to -5 dBm. An additional experiment was carried out to properly understand the reasons behind such performance reduction. Two adjacent tones at 3.47 and 3.5 GHz were coupled by an RF combiner and injected into the same RoF Tx module (Figure 3.2) in order to evaluate the nonlinear behavior of its RF amplifier, as well as that of the RoF Rx module. It is clear the generation of third-order intermodulation products in Figure 3.3a for -5 dBm power level for each initial tone. Afterward, only the 3.5 GHz carrier was transmitted with 30 MHz bandwidth at -2 dBm power. From Figure 3.3b, one can note that intermodulation products cause distortions in the RF modulated signal, implying an increase of noise floor, as in the previous case, and consequently, leading to a reduction in the signal-to-noise ratio (SNR).

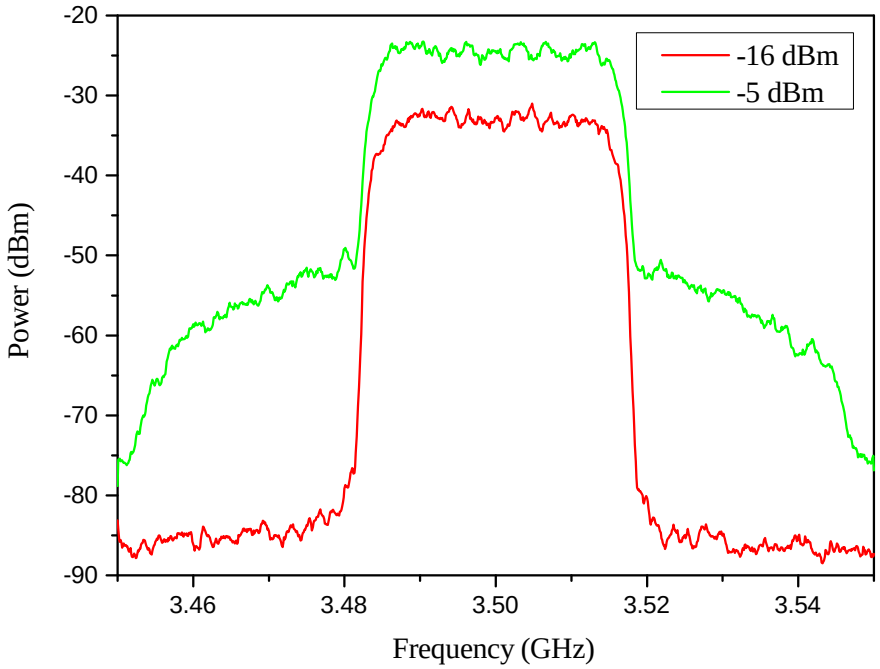

Figure 3.1: *Frequency spectrum in the RoF output for different RF input power.*

Subsequently, the spurious-free dynamic range (SFDR) parameter was analyzed in the RoF link to determine the threshold for the creation of intermodulation products. For this reason, the RF power at the RoF Tx module input has been increased until the generation of the intermodulation product and second harmonic (7 GHz) as reported in Figures 3.4a and 3.4b, respectively. It happened for a photodetected total power level

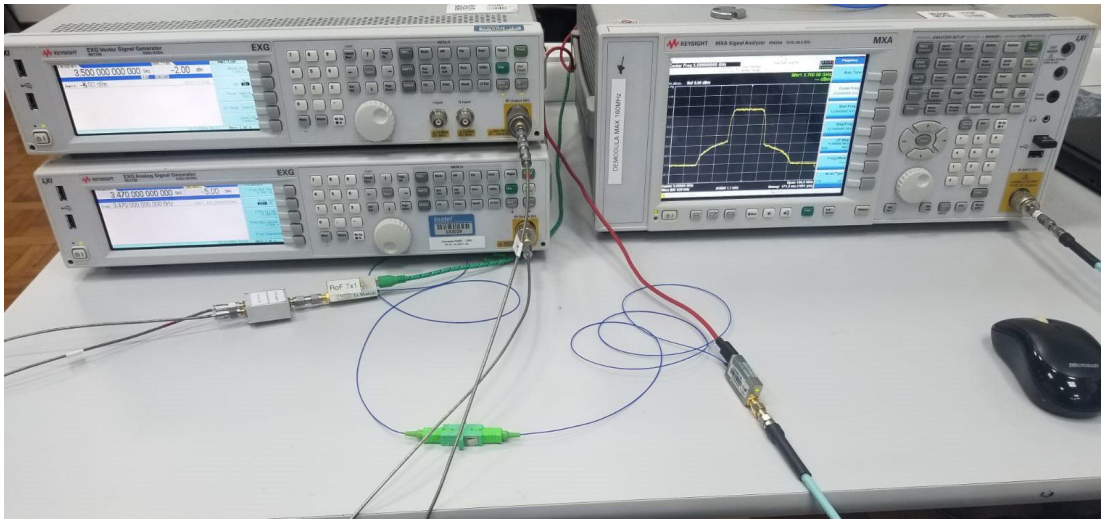

Figure 3.2: *Experimental setup for the intermodulation tests.*

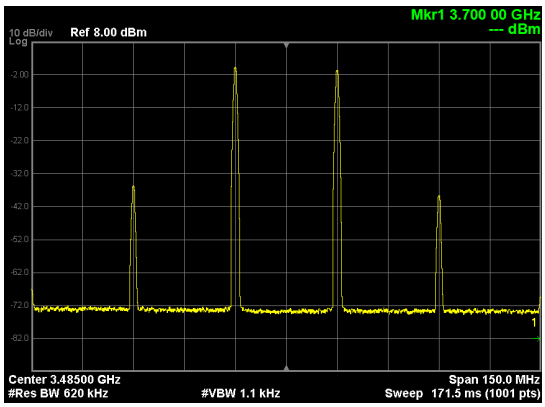

(a) *Spectrum with the two frequency tones and third-order intermodulation products.*

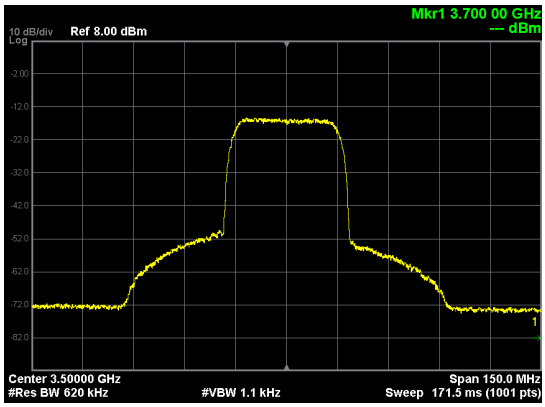

(b) *Distortions in the modulated signal caused by intermodulation products.*

Figure 3.3: *Generated intermodulation products in the RoF link.*

of -9.5 and -19.6 dBm, respectively. As a conclusion, the performance degradation noticed in the experiments from the Paper 1 can be associated with the saturation of RF amplifiers from the RoF modules operating in the nonlinear region, i.e. generating harmonics and intermodulation products, for high RF power levels.

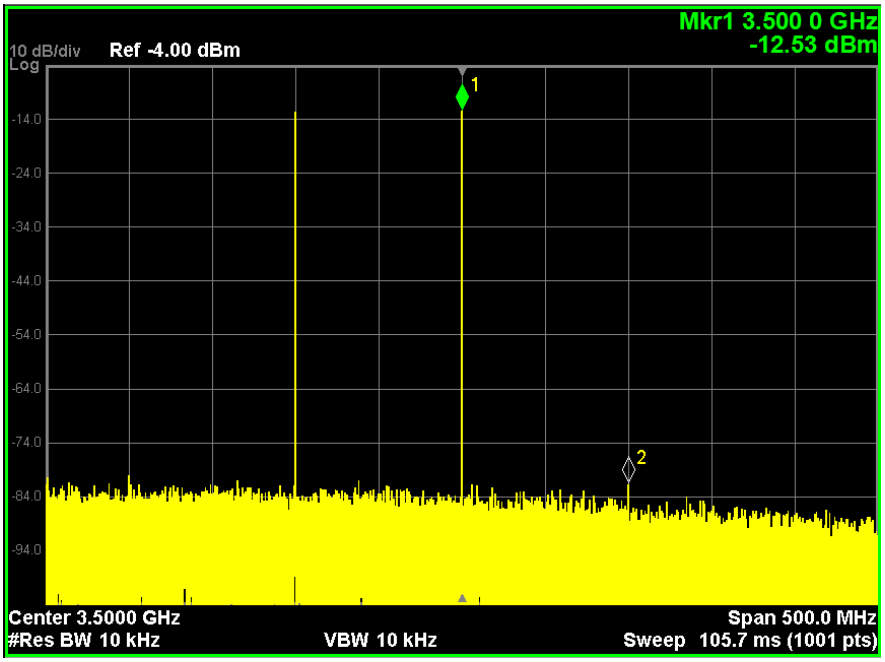

(a) *SFDR for the third-order intermodulation product.*

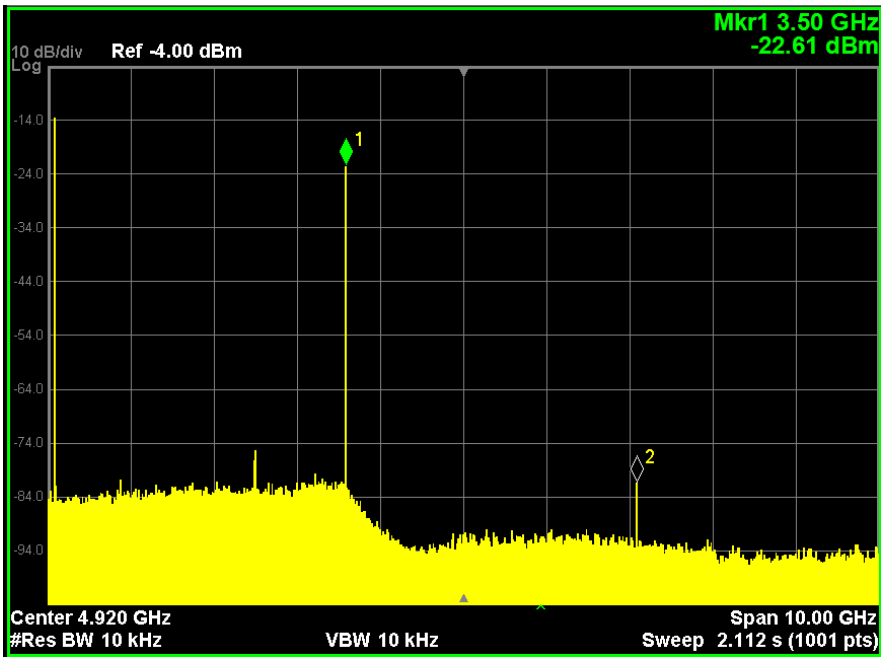

(b) *SFDR for the second harmonic signal.*

Figure 3.4: *Spurious-free dynamic range measurements in the RoF link.*

Paper 2: Optically-powered FiWi System for B5G Hybrid VLC/RF Access Networks

Felipe Batista Faro Pinto, Letícia Carneiro de Souza, Tomás Powell Villena Andrade, Eduardo Saia Lima, Rodnei Carçola, Evandro Lee Anderson, Francisco Martins Portelinha Junior and Arismar Cerqueira Sodré Junior. "*Optically-powered FiWi System for B5G Hybrid VLC/RF Access Networks*", submitted in *Optics Express*. **Publisher:** Optica

Optically-powered FiWi System for B5G Hybrid VLC/RF Access Networks

FELIPE B. F. PINTO,[1] LETICIA C. SOUZA,[1] TOMÁS P. V. ANDRADE,[1] EDUARDO S. LIMA, EVANDRO L. ANDERSON,[3] FRANCISCO M. P. JR.,[4] AND ARISMAR CERQUEIRA S. JR.[1]

[1] *Laboratory WOCA, National Institute of Telecommunications, 510 João de Camargo Avenue, Santa Rita do Sapucaí-MG, Brazil*
[2] *5G Innovation Office, VS Telecom, 616 Lord Cockrane Street, São Paulo-SP, Brazil*
[3] *MPTcable, Indaiatuba-SP, Brazil*
[4] *Inatel Competence Center (ICC), National Institute of Telecommunications, 510 João de Camargo Avenue, Santa Rita do Sapucaí-MG, Brazil*
[*] *felipe.pinto@dtel.inatel.br; arismar@inatel.br*

Abstract: This paper proposes the concept and reports the demonstrator of an optically-powered Fiber/Wireless (FiWi) system based on a hybrid visible light communication (VLC) and RF access network for beyond 5G (B5G) indoor applications. The power-over-fiber (PoF) technology is properly applied to simultaneously energize two components from the remote site, namely: a radio-over-fiber (RoF) module, which contains a photodetector and an RF amplifier; a red laser from the VLC system. A 500 m conventional multimode optical fiber (MMF) with 62.5 μm core diameter is used to transport 8.1 W optical power at a power transmission efficiency (PTE) of 14%. Regarding the communication setup, a 5G New Radio (5G NR) signal is initially transported through a RoF fronthaul, composed by 10 km of single mode fiber (SMF), followed by the hybrid VLC/RF access network. The performance investigation of the B5G communication system is based on analysis of the root mean square error vector magnitude (EVM_{RMS}) parameter. Experimental results indicate 1.2 Gbps throughput in the VLC link using a 200 MHz bandwidth and 64-quadrature amplitude modulation (64-QAM), resulting in approximately 4.02% of EVM_{RMS}. Moreover, the RF link at 3.5 GHz provides 360 Mbps with EVM_{RMS} of 2.67%. Finally, a comparison between the PoF system and conventional power supply validates the proposed approach applicability for B5G wireless communications.

1. Introduction

The fifth generation of mobile networks (5G) has been commercialized worldwide in the last years for covering three main application scenarios [1, 2]: enhanced mobile broadband (eMBB); ultra-reliable and low latency communications (URLLC); massive machine-type communications (mMTC). In parallel, the sixth-generation of mobile networks (6G) [3–5] is already under study, envisaging higher security and privacy, lower energy consumption and extremely large bandwidth compared with 5G. The radio-over-fiber (RoF) technology plays an important role in fulfilling those requirements, by means of conciliating the extremely wide bandwidth and electromagnetic interference immunity from optical systems with the flexibility and mobility from the mobile communications systems [6, 7]. Essentially, an RoF link consists of transporting radio frequency (RF) signals through fiber-optic links, making it an interesting solution not only for the core network, but also for backhaul, midhaul and fronthaul. Particularly, the centralized-radio access network (C-RAN) architecture allows to simplify the base stations (BS) and reduces its energy consumption, by centralizing and processing all baseband signals in the Central Office (CO) [8]. In addition, analog radio-over-fiber (A-RoF) arises with the advantage of transmitting passband signals through the fiber-optics fronthauls, eliminating costs with analog to digital conversions and frequency upconversion and downconversion in the base stations [9].

Regarding the access network, the radio frequency (RF) wireless system is the most common

approach to attend to the plethora of users, which combined with an optical fronthaul composes a fiber-wireless (FiWi) system. Nevertheless, other technologies have emerged as alternatives to complement conventional RF wireless links. For instance, visible light communication (VLC) is a type of optical wireless communication (OWC) that appears with great potential for the beyond 5G (B5G) and 6G networks, by offering larger bandwidths compared to millimeter-waves (mm-waves), as well as high security and electromagnetic interference immunity to the RF signals present in the environment [10]. Particularly, the VLC systems have been recognized as a key enabling technology for 6G, due to its remarkable advantages, namely [11]: terahertz level bandwidth, unlicensed spectrum, easy integration to fiber-optic links, energy efficiency, low-cost compared to THz communications, no electromagnetic interference and high-frequency reuse. The VLC technology has been largely proposed for indoor applications, not only offices, but also hospitals, industry and airplanes, which are typically very critical in terms of interference [12]. Additionally, VLC can also be implemented in outdoor scenarios, such as vehicle-to-vehicle (V2V), road-to-vehicle (R2V) and building-to-building (B2B) communications [13].

Another promising technique involves transmitting high optical power levels through optical fibers, with the purpose of energizing some low-power components located in remote areas or in harsh environments. This technique, known as power-over-fiber (PoF), is typically composed by three main components: a high-power laser diode (HPLD) that provides high optical power; an optical fiber for transmitting the optical beams; a photovoltaic power converter (PPC) for converting energy from the optical to the electrical domain. PoF systems provide some advantages over the use of cooper wires, such as low loss, electromagnetic interference immunity, low weight, and galvanic isolation [14, 15]. These characteristics make PoF an interesting solution to supply components from mines, factories and other harsh environments [16]. The specialized literature presents PoF systems applied to different scenarios using different types of optical fiber. For instance, in [17], authors have implemented a PoF system based on a single-mode fiber (SMF) to simultaneously transmit power and data, aiming for 5G networks and Internet of Things (IoT) applications. A 2-W optical power centered at 1480 nm was transmitted along with a 5G New Radio (5G NR) signal over 10 km of an SMF, obtaining 870 mW at the demultiplexer end. In [18], H. Yang et al reported a co-transmission of 10-W optical power with a 5G NR signal throughout a 1-km SMF link, collecting 7.18 W of received optical power. Moreover, one can easily find many PoF system implementations using multimode fibers (MMFs) [19–22]. In particular, our research group have used 100 m MMF with 105-μm core diameter in a dedicated link to transmit 2.2 W optical power in order to feed a RoF module from in a SMF based-5G NR system [19]. A dedicated 300 m MMF link with 200 μm of core diameter was used to transmit 1.5 W in [20]. 360 mW was obtained after the optical-electrical conversion, which was used to feed a proximity sensor for hazardous environment applications. In [21], a 4 km MMF link with 62.5 μm of core diameter was used in a shared scenario, by transmitting 10 W optical power with a 5G NR signal in the same MMF link. The center-launching (CL) and offset-launching (OL) techniques were used to mitigate the modal dispersion and crosstalk interference for the co-transmission, collecting 6 W of output optical power. Meanwhile, in [22], a 300 m MMF with 62.5 μm of core diameter was implemented to transmit 250 mw optical power in order to feed a short-range remote unit.

There are also works based on the use of special optical fibers, such as double-clad fibers (DCFs) [23, 24] and multicore optical fibers (MCFs) [25] in the context of shared PoF systems. In [23], 150 W optical power provided by 4 HPLD was injected into the inner cladding from a 1 km DCF link, whereas a data signal was transmitted into its 8 μm core. A 7.08 W total electric power was obtained at the output of six PPCs. A DCF was also implemented in [24], in which a bidirectional communication system was deployed by transmitting data into the 9 μm core and 4 W optical power into the inner cladding, allowing to collect 400 mW at the output of two PPCs. In [25], 60 W optical power provided by six HPLDs was co-transmitted with a 5G NR

signal in a 1 km MCF link. By using six PPCs at the end of the PoF system, the authors achieved approximately 11.9 W in total. Table 1 presents the state-of-the-art regarding PoF system, including this work. It can be noted that the fiber type is a critical choice for each application. The DCF and MCF enable data transmission and high-power levels using the same fiber. However, due to their low availability and high complexity, they are very expensive. The SMF use could be considered a suitable choice for implementing PoF using an existent infrastructure, although its small core limits the optical power transmission. On the other side, MMFs provide much larger

Table 1. State-of-the-art on PoF systems.

Year/ Reference	**Powered Device**	**Application/ Tx Power/ HPLD wavelength**	**Fiber type (core/clad)/ length(m)**	**Electrical output power (W)**	**PPC efficiency/ PTE (%)**	**Wireless communication standard/Reach(m)**	**Throughput (Gbps)**
2021/ [18]	None	Transmitting simultaneously power and data in a same SMF fiber/ 10 W/1064.8 nm	SMF(8.2/125 μm)/ 1000	-	-	5G NR/ not applicable	1.5
2021/ [17]	None	Transmitting simultaneously power and data in a same SMF fiber aiming for IoT applications/ 2 W/1480 nm	SMF(8.2/125 μm)/ 10000	-	-	5G NR/ 0.7	0.2*
2020/ [23]	None	Transmitting simultaneously power and data in a same DCF fiber/ 150 W/808 nm	DCF(8/125 μm)/ 1000	7.08	24/4.84	IEEE 802.11a/ not applicable	-
2015/ [24]	None	Transmitting simultaneously power and data in a same DCF fiber/ 4 W/830 nm	DCF(9/105 μm)/ 100	0.4	28.6/10*	IEEE 802.11g/ not applicable	0.054
2022/ [25]	None	Transmitting simultaneously power and data in a same MCF fiber/ 60 W/1064.8 nm	MCF(9/150 μm)/ 1000	-	-	5G NR/ not applicable	9
2022/ [19]	RoF module (photodetector and a electrical amplifier)	Feeding a RoF module in a 5G NR network/ 2.2 W/975 nm	MMF(100/140 μm)/ 100	0.516	30/23.5	5G NR/ 10	0.5
2018/ [20]	Proximity sensor	Feeding a proximity sensor for hazard environment applications/ 1.5 W/808 nm	MMF(200/500 μm)/ 300	0.36	52/24*	not applicable	-
2018/ [21]	None	Transmitting simultaneously power and data in a same MMF fiber/ 10 W/1550 nm	MMF(62.5/125 μm)/ 4000	-	-	IEEE standard/ not applicable	0.054
2008/ [22]	Short range remote unit (laser, photodector, electrical amplifier)	Feeding a short range remote unit/ 250 mW/834 nm	MMF(62.5/125 μm)/ 300	0.1*	50/40*	IEEE 802.11g/ not applicable	0.054
This work	VLC laser and a RoF module (photodetector and a electrical amplifier)	Feeding a RoF module and VLC laser, aiming indoor 5G NR communications/ 8.1 W/808 nm	MMF(62.5/125 μm)/ 500	1.06	23.75/14	5G NR/ 3	1.2

*The presented value was calculated from the corresponding reference.

cores compared to SMFs, allowing much higher optical power levels, and keeping low-cost as well. However, despite that advantage, the use of MMFs with non-conventional large cores (100, 105, or even 200 μm) makes their implementation more difficult in existent optical networks. In contrast, the 62.5-μm core MMF is a standardized and broadly commercialized fiber, making it very attractive for PoF systems.

To the best of our knowledge, this paper presents, for the first time in literature, the concept and implementation of an optically-powered FiWi system for B5G hybrid VLC/RF access networks, by applying PoF technology with conventional 62.5 μm-core MMF. It is also worth mentioning that most works on PoF from literature do not feed any telecom component at the remote side, while we properly energize two different devices (a RoF module and a VLC red laser) using a single PPC in the current work.

The application scenario might be seen in Fig. 1. This scenario represents the proposed optically-powered FiWi system for B5G hybrid VLC/RF access networks applied to two different environments, i.e. a hospital and an industry. In both cases, the VLC and RF access networks are complementary, since offices, rooms and reception can be covered by conventional RF networks, whereas communications in electromagnetically sensitive environments, such as ICUs (intensive care units) at hospitals and factory floors at industries are ensured by using VLC links.

The paper is structured in five sections. Section 2 presents the PoF experimental setup and its characterization in terms of efficiency and stability. Section 3 describes the first phase on the implementation of the proposed optically-powered FiWi system for B5G, which is based on the integration of an optical fronthaul based on RoF technology followed by a VLC access network, both energized by the PoF system. The full implementation with a hybrid VLC/RF access network and its performance analysis are reported in Section 4. Finally, Section 5 outlines the conclusions and future works.

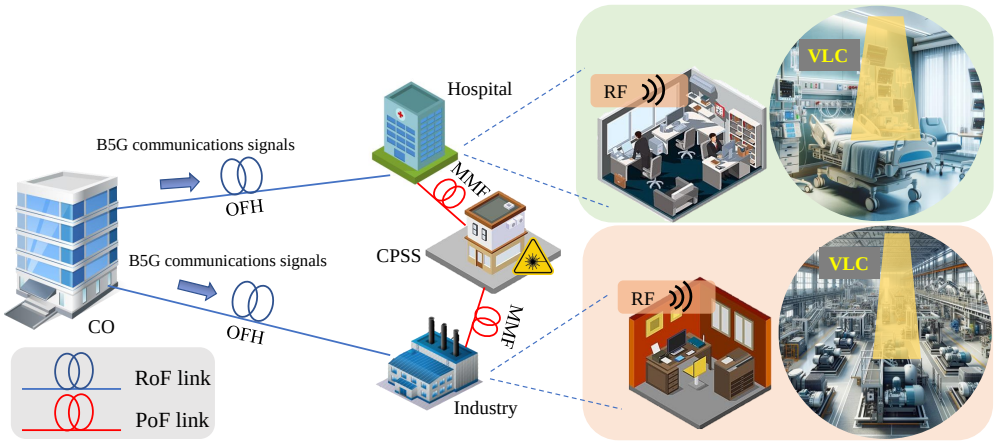

Fig. 1. Optically-powered FiWi system for B5G hybrid VLC/RF access networks towards 6G: CO- central office; B5G- beyond 5G; OFH- optical fronthaul; MMF - multimode fiber; CPSS- centralized power supply station; RF- radio frequency; VLC- visible light communication; RoF- radio-over-fiber.

2. PoF System Characterization

This section presents the PoF system experimental characterization. The PoF system was composed of an 808 nm HPLD that provides optical power up to 12W, a 500-m multimode fiber with a core diameter of 62.5 μm, a PPC that supports up to 20W of optical power and 23.75% of conversion efficiency at 808 nm, and two DC/DC converters with 85% of voltage efficiency. In

order to estimate the optical power transmission efficiency (OPTE), which indicates the relation between the output and input optical power of the system, an optical power meter was placed in the fiber end. Posterior, the PPC was connected to the fiber end to obtain the power transmission efficiency (PTE), which defines the relation between the output electric power and input optical power. For each optical power that is entering into the PPC, there is an optimal load that occurs the maximum power transfer. For this reason, a programmable DC electronic load was used to variate the load value for each optical power. The OPTE and PTE curves as a function of the optical input power are presented in Fig. 2(a) and Fig. 2(b), respectively. For HPLD optical powers levels from 1 up to 3 W, both curves presented lower efficiency before the stability, which may be associated with the low HPLD efficiency at small optical powers. From 4 W and on, the measured OPTE was approximately 60%, whilst PTE stabilizes at about 14%.

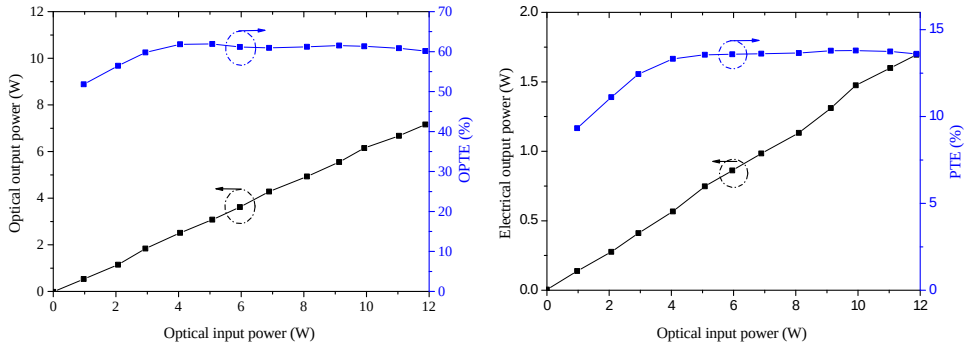

(a) Optical power transmission efficiency. (b) Power transmission efficiency.

Fig. 2. Efficiency curves of the PoF system.

Afterward, the optical and electrical stability of the PoF system was measured over 1 hour, as reported in Fig. 3. For this test, the input optical power was set at a level enough to feed the RoF module and VLC laser. The VLC and RoF setups will be discussed into details in the next section. From Fig. 3, one can observe an excellent stability for both curves, maintaining a mean

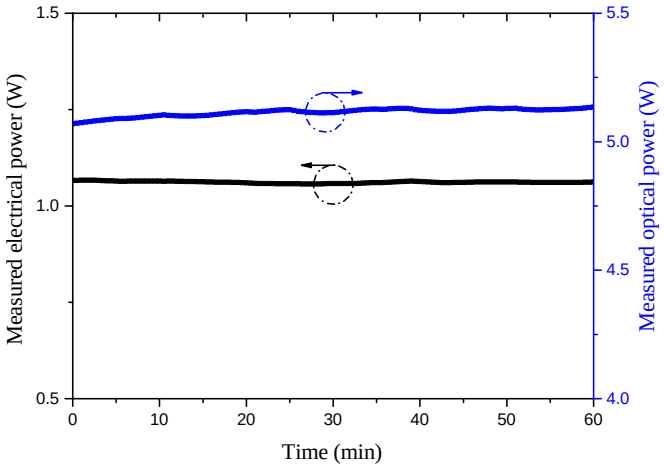

Fig. 3. PoF system stability test over one hour.

value of 5.11 W with a standard deviation of 0.017 for the optical power and a mean value of 1.06 W with a standard deviation of 0.003 for the electrical power. Such stability is ensured by the large passive sink mounted on the PPC and thermoelectric cooler (TEC) from HPLD.

3. Optically-Powered VLC/RoF System

This section aims to realize a preliminary performance analysis of the RoF-based fronthaul with the VLC access network, both powered by the PoF system, as illustrated in Fig 4. An arbitrary waveform generator (AWG) (model M8190A) and an RF generator (model PSG E8267D), both from Keysight, were used to generate a baseband signal and upconvert it to 650 MHz, respectively. The upconversion process was implemented to adequate the RF signal central frequency to operate within the standardized 5G NR frequency range 1 (FR1). The upconverted signal was injected into the RF input from the RoF Tx module, which is composed of a 20 dB gain electric amplifier (EA) and a laser diode (LD). The 4 dBm optical signal, centered at 1550 nm and generated by direct modulation, was transmitted through a 10 km SMF link (RoF-based fronthaul), converted to the electrical domain by using a photodetector (PD) and amplified by an additional 20 dB gain electrical amplifier, both from the same RoF Rx module. The obtained RF signal was sent to the VLC module, composed by a red LD and a bias tee (BT). Another TEC was used for the red laser for keeping the temperature at 25°C. An achromatic lens was placed at the end of the 3 m-VLC link to focus the light beam into a silicon-based photodetector. The electrical output signal from PD was sent to another BT in order to reject the DC component and exclusively analyzing the RF frequencies. Finally, the RF signal was analyzed and demodulated by a signal and spectrum analyzer from Rohde & Schwarz (Model FSW67). Regarding the PoF system, two DC/DC converters were connected in parallel at the PPC output for adjusting the voltage level. The first one was used to feed the RoF Rx module, by reducing the voltage from 18 V to 5 V. On the other hand, the second DC/DC converter was adjusted to provide about 3V and 20 mA for properly powering the VLC red laser. Each communication system (RoF and VLC) with its correspondent DC/DC converter was individually characterized. The root mean square error

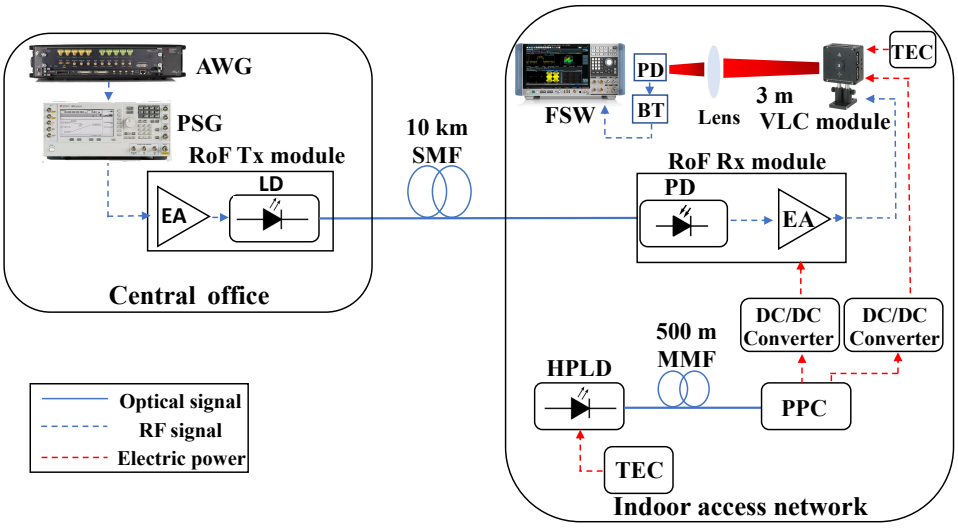

Fig. 4. Block diagram of the optically-powered hybrid VLC/RoF system: AWG- arbitrary waveform generator; EA- electrical amplifier; LD- laser diode; SMF- single-mode fiber; PD- photodiode; HPLD- high-power laser diode; TEC- thermoelectric cooler; PPC- photovoltaic power converter; BT- bias tee.

vector magnitude (EVM_{RMS}) was used as the performance metric. The EVM_{RMS} describes the mean value of the difference between the vectors of the ideal location and received symbols.

Using the baseband signal generated by AWG, the IQ Tools software was applied to create digital signals with different modulation orders, such as quadrature phase shift keying (QPSK), 16-quadrature amplitude modulation (QAM) and 64-QAM. The PSG upconverted the digital signal to 650 MHz, which corresponds to the VLC module optimal response within FR1. In the first phase, a 200 MHz bandwidth RF signal obtained by the RoF Rx module was directly evaluated by FSW, i.e. without passing through the VLC link. Posterior, the VLC system was inserted after the RoF link, as the access network. Fig. 5(a) reports the EVM_{RMS} measurements of the RoF system as a function of the fronthaul RF input power with QPSK, 16-QAM and 64-QAM. The 3rd Generation Partnership Project (3GPP) Release 18 [26] establishes the maximum allowed EVM_{RMS} for each modulation order, as represented by the colored horizontal lines from the graph: 17.5%, 12.5%, and 8% for QPSK, 16-QAM, and 64-QAM, respectively. It may be noted the optically-powered RoF system satisfies the 3GPP limits for the entire power level range when using QPSK and 16-QAM. Particularly for 64-QAM, the performance is in accordance to the 3GPP requirement for power levels higher than approximately - 42dBm. The EVM_{RMS} values of the optically-powered VLC/RoF system as a function of the fronthaul RF input power might be seen in Fig. 5(b). Different bandwidths were set for the RF signal with 64-QAM modulation order. The system performance for 60 and 100 MHz bandwidth is very similar, attending the 3GPP requirement for power levels higher than -32 dBm, requiring about 18 dB of additional power when compared to the previous case. This power penalty is explained by the intrinsic loss from the 3-m long VLC system, including the electrical-optical and optical-electrical conversions, as well as the free-space and coupling losses. For 200 MHz bandwidth, it is required -23 dBm to accomplish the 3GPP requirement, as a result of the larger bandwidth. Moreover, it is important to comment on the upward behavior observed for powers at nearly -21 dBm and -12.5 dBm in Fig. 5(a) and Fig. 5(b), respectively. Such behavior may be associated with the electrical amplifier saturation from the RoF Rx module. The amplifier reaches the 1 dB compression point and starts to operate in the nonlinear region. Consequently, unwanted effects start to appear, such as distortions, harmonics and intermodulation products.

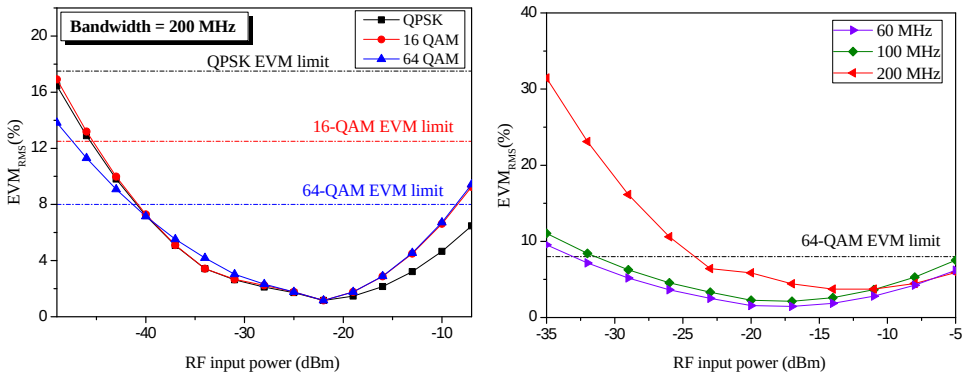

(a) PoF-based RoF system. (b) PoF-based VLC/RoF system.

Fig. 5. Performance analyses of the optically-powered RoF and VLC systems as a function of the fronthaul RF input power.

In addition, Fig. 6 presents a performance comparison between the optically-powered system and a conventional power supply, with the purpose of validating the proposed PoF system. A 64-QAM 5G NR signal with a 60 MHz bandwidth was configured to be transmitted over the

VLC/RoF-based system, powered either by the PoF system or conventional electrical power supplies. As can be observed, both curves exhibit very similar behavior, with a higher discrepancy at lower RF input powers, approximately 4% difference at -44 dBm, and tend towards the same best EVM_{RMS} value of about 2%.

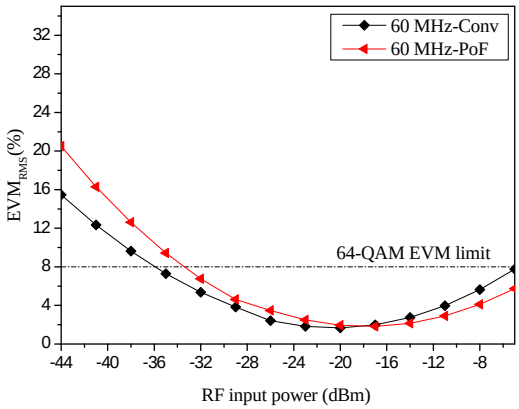

Fig. 6. Experimental performance comparison between the optically-powered and conventional systems.

4. Optically-Powered FiWi System with Hybrid VLC/RF Access Networks

In the final implementation, a 3 m-RF wireless link was added to demonstrate the simultaneous operation of PoF-based VLC and RF access networks for B5G applications, as described in Fig. 7. A vector signal generator (model EXG N5172B) from Keysight was utilized to generate the second RF signal of the proposed FiWi system. A 2-way electric coupler was used to combine the PSG and EXG signals for exciting the RoF Tx module, which was coupled to the SMF link. At the SMF link output, a variable optical attenuator (VOA) and an optical power monitor (OPM) were set to vary and monitor the optical power, respectively. The electric combined signal at the RoF Rx module output was divided by a 2-way electric splitter. One port was connected to the VLC module and the other one was to excite a tri-band antenna array with 9 dBi gain, previously developed by our research group [27]. Since there were two data signals in the system, a signal

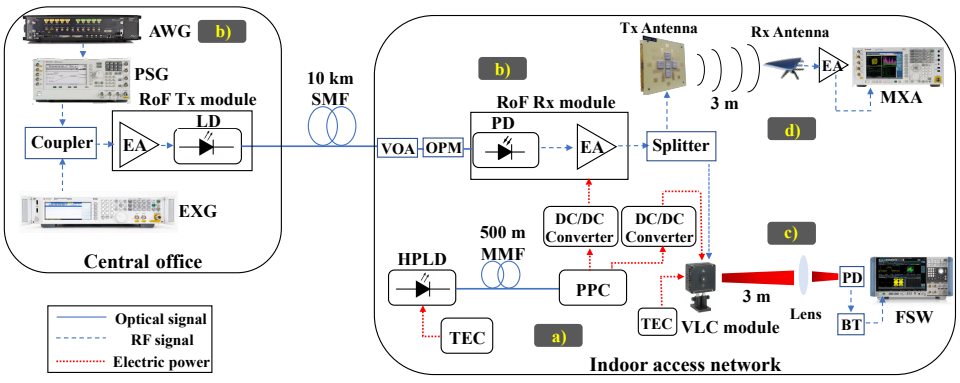

Fig. 7. Block diagram of the optically-powered FiWi system with hybrid VLC/RF Access Networks: VOA- variable optical attenuator; OPM- optical power monitor.

analyzer from Keysight (model MXA N9020A) was utilized in the final setup. Fig. 8 presents photographs of the experimental setup with all components and pieces of equipment, labeled accordingly to the schematic from Fig. 7.

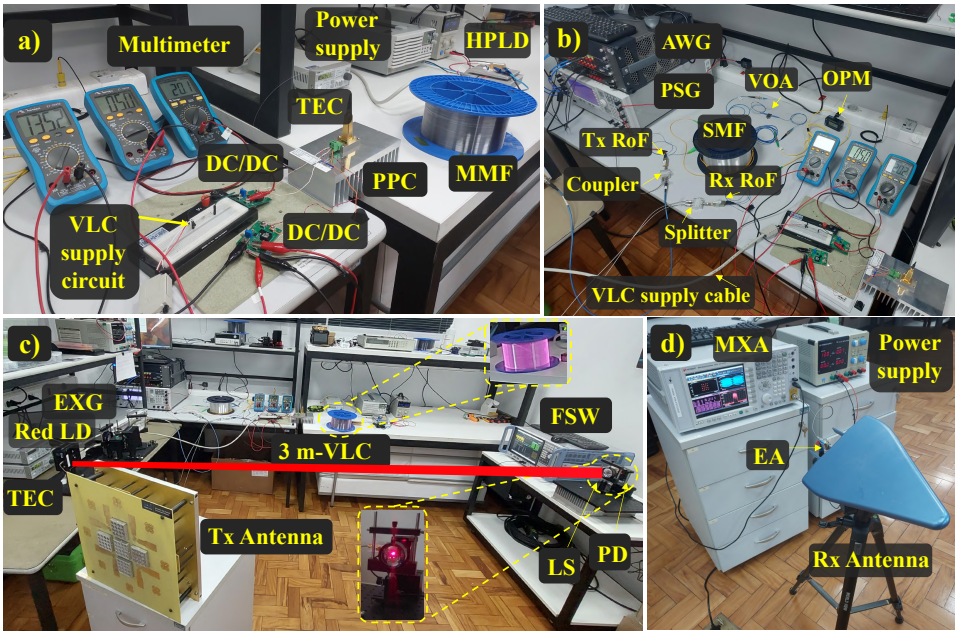

Fig. 8. Photograph of the entire experimental setup: a) PoF system; b) RoF system; c) VLC link and transmitting antenna; d) Receiver setup and receiving antenna.

First, PSG was set to upconverter the 5G baseband signal to 650 MHz for the VLC link, whilst a 3.5 GHz signal with 25-MHz bandwidth and 64-QAM was configured in EXG for the conventional RF wireless link. Fig. 9(a) reports the EVM_{RMS} as a function of the RF input power for three different conditions of the VLC system (60, 100, and 200 MHz bandwidth). For all analyzed bandwidths the VLC system performance accomplishes the 3GPP requirement with

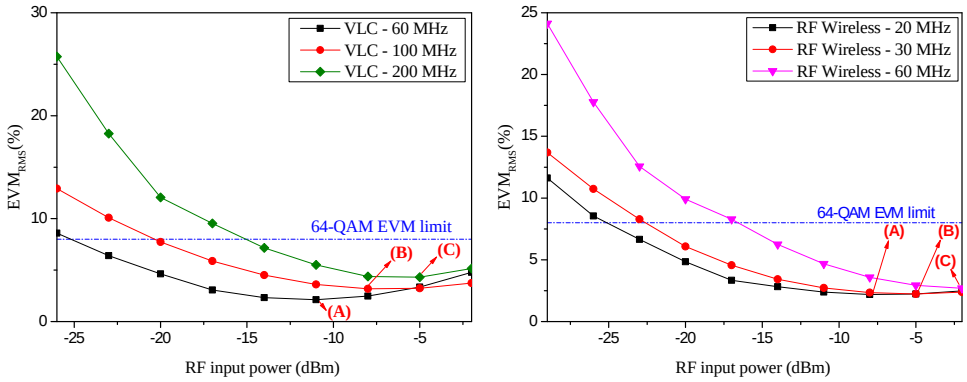

(a) VLC link. (b) RF wireless link.

Fig. 9. Performance analysis of the optically-powered FiWi system with hybrid VLC/RF access networks.

margin for RF input power higher than -15 dBm. The best obtained EVM_{RMS} parameter varied from 1.93% to 4.02% for 60, 100, and 200 MHz bandwidth, when the proposed system achieved 1.2 Gbps throughput in the VLC link.

Afterward, the PSG upconverted the 5G signal to 3.5 GHz to be transmitted through the RF wireless link in conjunction with a 64 QAM 35-MHz bandwidth signal from the VLC link. The 5G NR signal bandwidth in the RF wireless link was configured to 20, 30, and 60 MHz, and the EVM_{RMS} results might be seen in Fig. 9(b). A throughput of 260 Mbps with 2.67% of EVM_{RMS} was achieved for the 5G NR signal in the RF wireless link. For each curve from Fig. 9, the best-attained performance, i.e. the lowest EVM_{RMS} for each evaluated case, was labeled as A, B, and C. The obtained spectrum and constellation of the signals for each one of those labels are displayed in Fig. 10(a) and Fig. 10(b). As expected, as the 5G NR signal bandwidth is increased, more distortions are observed in the measured constellations, due to more errors from the received symbols amplitude and phase. In any case, all constellations are clear with EVM_{RMS} within the thresholds limited by the 3GPP.

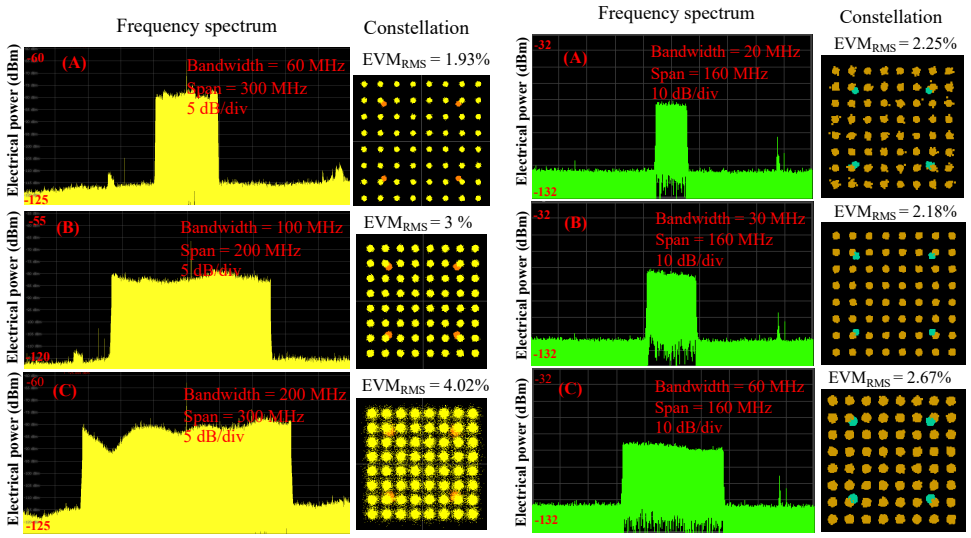

(a) VLC link-based 5G NR system.

(b) RF wireless link-based 5G NR system.

Fig. 10. Frequency spectra and constellations of the optically-powered FiWi system for B5G hybrid VLC/RF access networks.

5. Conclusions

We have proposed and efficiently implemented an optically-powered FiWi system for B5G indoor applications with a hybrid VLC/RF access network. The deployed PoF system enabled to simultaneously energize two loads, i.e. a RoF module (photodetector and an electrical amplifier) and a VLC laser, using a single PPC. More specifically, a 500-m 62.5 μm-core MMF link was used to transmit 8.11 W, collecting approximately 1.06 W at the PPC output, achieving an OPTE and PTE of 60% and 14%, respectively. Additionally, the PoF system has characterized in terms of stability over a period of an hour. The optical power has been kept constant with a mean value of 5.11 W with a standard deviation of 0.017, whereas the respective values for the electrical power were 1.06 W and 0.003, respectively. Such stability was ensured by using a large passive sink mounted on the PPC and a thermoelectric cooler for HPLD.

Two different optical wireless communication architectures were deployed to demonstrate

the applicability of the proposed PoF-based approach, namely: an optically-powered VLC/RoF system; an optically-powered FiWi System with Hybrid VLC/RF access networks. In both, a 10-km long SMF link was applied as a fronthaul using the RoF technology. The EVM_{RMS} was used as a performance metric to evaluate the 5G NR performance. A throughput of 1.2 Gbps was achieved in the VLC link with a 200 MHz bandwidth and 64-QAM modulation, resulting in approximately 4.02% of EVM_{RMS}. Whereas in the RF wireless link, 360 Mbps was obtained with 2.67% of EVM_{RMS} for a 60 MHz bandwidth with 64-QAM. For validation purposes, a comparison between the optically-powered system and conventional electric power supply was carried out, which indicated a similar behavior, validating the proposed PoF system performance and its applicability for B5G networks. Future works regards the use of other OWC technologies, including free space optical (FSO), as well as the implementation of 5G-NR FiWi systems operating in mm-waves.

Funding

This work received partial funding from Project XGM-AFCCT-2024-2-15-1, supported by xGMobile – EMBRAPII-Inatel Competence Center on 5G and 6G Networks, with financial resources from the PPI IoT/Manufacturing 4.0 program of MCTI (grant number 052/2023), signed with EMBRAPII. The authors also thank the financial support from CNPq, CAPES, FINEP, FAPEMIG (Contracts # PPE-00124-23, RED-00194-23 and APQ-02746-21), FAPESP (Contracts # 2021/06569-1 and # 2022/09319-9), and MPT cable.

References

1. J. Navarro-Ortiz, P. Romero-Diaz, S. Sendra, *et al.*, "A survey on 5G usage scenarios and traffic models," IEEE Commun. Surv. & Tutorials **22**, 905–929 (2020).
2. M. Shafi, A. F. Molisch, P. J. Smith, *et al.*, "5G: A tutorial overview of standards, trials, challenges, deployment, and practice," IEEE journal on selected areas communications **35**, 1201–1221 (2017).
3. S. Dang, O. Amin, B. Shihada, and M.-S. Alouini, "What should 6G be?" Nat. Electron. **3**, 20–29 (2020).
4. M. Latva-Aho, K. Leppänen *et al.*, "Key drivers and research challenges for 6G ubiquitous wireless intelligence," (2019).
5. W. Saad, M. Bennis, and M. Chen, "A vision of 6G wireless systems: Applications, trends, technologies, and open research problems," IEEE network **34**, 134–142 (2019).
6. J. Beas, G. Castanon, I. Aldaya, *et al.*, "Millimeter-wave frequency radio over fiber systems: a survey," IEEE Commun. surveys & tutorials **15**, 1593–1619 (2013).
7. E. S. Lima, R. M. Borges, N. Andriolli, *et al.*, "Integrated optical frequency comb for 5G NR Xhauls," Sci. Reports **12**, 16421 (2022).
8. H. R. D. Filgueiras, E. S. Lima, M. S. B. Cunha, *et al.*, "Wireless and optical convergent access technologies toward 6G," IEEE Access **11**, 9232–9259 (2023).
9. J. P. Santacruz, "Analog Radio-over-Fiber for 5G/6G Millimeter-Wave Communications," TU/e (2022).
10. G. Gui, M. Liu, F. Tang, *et al.*, "6G: Opening new horizons for integration of comfort, security, and intelligence," IEEE Wirel. Commun. **27**, 126–132 (2020).
11. S. Soderi and R. De Nicola, "6G networks physical layer security using RGB visible light communications," IEEE Access **10**, 5482–5496 (2021).
12. L. Feng, R. Q. Hu, J. Wang, *et al.*, "Applying VLC in 5G networks: Architectures and key technologies," Ieee Netw. **30**, 77–83 (2016).
13. A. R. Ndjiongue and H. C. Ferreira, "An overview of outdoor visible light communications," Trans. on Emerg. Telecommun. Technol. **29**, e3448 (2018).
14. J. D. L. Cardona, P. C. Lallana, R. Altuna, *et al.*, "Optically feeding 1.75 W with 100 m MMF in efficient C-RAN front-hauls with sleep modes," J. Light. Technol. **39**, 7948–7955 (2021).
15. L. C. Souza, E. R. Neto, E. S. Lima, and A. C. S. Junior, "Optically-powered wireless sensor nodes towards industrial internet of things," Sensors **22**, 57 (2021).
16. R. H. Souza, P. Kiohara, L. Ghisa, *et al.*, "Analog response in optically powered radio-over-fiber links with distributed amplification in single-mode fibers," J. Light. Technol. (2023).
17. F. M. Al-Zubaidi, J. L. Cardona, D. S. Montero, and C. Vazquez, "Optically powered radio-over-fiber systems in support of 5G cellular networks and IoT," J. Light. Technol. **39**, 4262–4269 (2021).
18. H. Yang, D. Peng, Y. Qin, *et al.*, "10-W power light co-transmission with optically carried 5G NR signal over standard single-mode fiber," Opt. Lett. **46**, 5116–5119 (2021).

19. L. C. de Souza, E. S. Lima, and A. C. S. Junior, "Implementation of a full optically-powered 5G NR fiber-wireless system," IEEE Photonics J. **14**, 1–8 (2022).
20. J. D. López-Cardona, C. Vázquez, D. S. Montero, and P. C. Lallana, "Remote optical powering using fiber optics in hazardous environments," J. Light. Technol. **36**, 748–754 (2017).
21. H. Kuboki and M. Matsuura, "Optically powered radio-over-fiber system based on center-and offset-launching techniques using a conventional multimode fiber," Opt. Lett. **43**, 1067–1070 (2018).
22. D. Wake, A. Nkansah, N. J. Gomes, *et al.*, "Optically powered remote units for radio-over-fiber systems," J. Light. Technol. **26**, 2484–2491 (2008).
23. M. Matsuura, N. Tajima, H. Nomoto, and D. Kamiyama, "150-w power-over-fiber using double-clad fibers," J. Light. Technol. **38**, 401–408 (2019).
24. M. Matsuura and J. Sato, "Bidirectional radio-over-fiber systems using double-clad fibers for optically powered remote antenna units," IEEE Photonics J. **7**, 1–9 (2014).
25. H. Yang, S. Wang, D. Peng, *et al.*, "Optically powered 5G WDM fronthaul network with weakly-coupled multicore fiber," Opt. Express **30**, 19795–19804 (2022).
26. "3GPP TS 38.141-1. Base Station conformance testing, Part 1: Conducted conformance testing, Release 18." (2023).
27. T. Brandão and A. Cerqueira, "Triband Antenna Array for FR1/FR2 5G NR Base Stations," IEEE Antennas Wirel. Propag. Lett. **22**, 764–768 (2022).

3.2 Complementary discussions on the Paper 2

This section is regarding the circuits used to adjust the electrical output (voltage and current) of the PPC utilized in the PoF experiments from Paper 2. Figure 3.5 presents the electric circuits responsible for feeding the RoF Rx module and VLC laser, using two DC/DC converters. For the RoF Rx module, the only adjustment was setting its DC/DC converter to 5V. On other hand, for the VLC laser, it was necessary to add a 150 Ω resistor in series with its DC/DC for ensuring 20 mA current.

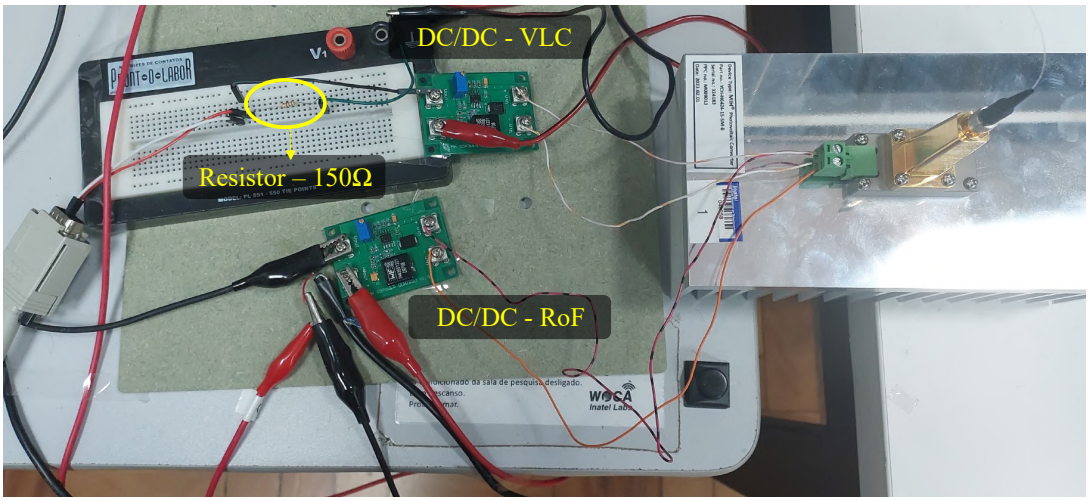

Figure 3.5: *Implemented electric supply circuit.*

Chapter 4

Conclusions and Futures Works

This dissertation reported two implementations of PoF systems applied to 5G/6G networks, focused on evaluating its applicability to optically feeding a mobile communication system. In Chapter 1, the contextualization and motivation were presented, as well as a literature review on the PoF technology, including the use of different optical fiber types as a transmission medium for transporting not only data, but also power.

Chapter 2 concerns a technical background on the PoF and VLC technologies. Moreover, it presented characterizations of their main components, such as HPLD, PPC, and VLC laser. In addition, the highlights of the two implemented optically-powered 5G/6G networks (Chapter 3) were described. In the first implementation, the PoF technique was successfully deployed to power a RoF Rx module from a 5G NR system with 50-MHz bandwidth and different modulation schemes. A 5W optical power was transmitted over a 100-m conventional MMF link before reaching PPC, implying in PTE= 19%. A performance analysis, as a function of the EVM_{RMS} parameter and in accordance to 3GPP requirements, and a comparison between the PoF and a conventional electrically-powered RoF system demonstrated the feasibility of optically powering the proposed 5G NR for 600 Mbps throughput in the context of industrial applications.

In the second implementation, it was proposed and efficiently implemented an optically-powered FiWi system for B5G indoor applications with a hybrid VLC/RF access network. The deployed PoF system enabled to simultaneously energize two loads, i.e. a RoF module (photodetector and an electrical amplifier) and a VLC laser, using a single PPC. More specifically, a 500-m 62.5 μm-core MMF link was used to transmit 8.11 W, collecting approximately 1.06 W at the PPC output, achieving an OPTE and PTE of 60% and 14%, respectively. Additionally, the PoF system is characterized in terms of stability over a period of an hour. The optical power has been kept

constant with a mean value of 5.11 W with a standard deviation of 0.017 W, whereas the respective values for the electrical power were 1.06 W and 0.003 W, respectively. Such stability was ensured by using a large passive sink mounted on the PPC and a thermoelectric cooler for HPLD.

Subsequently, two different optical wireless communication architectures were deployed to demonstrate the applicability of the proposed PoF-based approach, namely: an optically-powered VLC/RoF system; an optically-powered FiWi System with Hybrid VLC/RF access networks. In both, a 10-km long SMF link was applied as a fronthaul using the RoF technology. The EVM_{RMS} was used as a performance metric to evaluate the 5G NR performance. A throughput of 1.2 Gbps was achieved in the VLC link with a 200 MHz bandwidth and 64-QAM modulation, resulting in approximately 4.02% of EVM_{RMS}. Whereas in the RF wireless link, 360 Mbps was obtained with 2.67% of EVM_{RMS} for a 60 MHz bandwidth with 64-QAM. For validation purposes, a comparison between the optically-powered system and conventional electric power supply was carried out, which indicated a similar behavior, validating the proposed PoF system performance and its applicability for B5G networks.

Future works regard the application of PoF systems to B5G systems based on other OWC technologies, including free-space optical (FSO), as well as the implementation of 5G-NR FiWi systems operating in mm-waves. Moreover, it is proposed to implement PoF systems based on shared-scenarios, in which either data and power are transmitted using the same optical fiber. The latter approach could also take place in free space, using lenses and dichroic filters.

References

[1] J. Navarro-Ortiz, P. Romero-Diaz, S. Sendra, P. Ameigeiras, J. J. Ramos-Munoz, and J. M. Lopez-Soler, "A survey on 5G usage scenarios and traffic models," *IEEE Communications Surveys & Tutorials*, vol. 22, no. 2, pp. 905–929, 2020.

[2] M. Shafi, A. F. Molisch, P. J. Smith, T. Haustein, P. Zhu, P. De Silva, F. Tufvesson, A. Benjebbour, and G. Wunder, "5G: A tutorial overview of standards, trials, challenges, deployment, and practice," *IEEE journal on selected areas in communications*, vol. 35, no. 6, pp. 1201–1221, 2017.

[3] N. Al-Falahy and O. Y. Alani, "Technologies for 5G networks: Challenges and opportunities," *It Professional*, vol. 19, no. 1, pp. 12–20, 2017.

[4] X. Ge, S. Tu, G. Mao, C.-X. Wang, and T. Han, "5G ultra-dense cellular networks," *IEEE Wireless Communications*, vol. 23, no. 1, pp. 72–79, 2016.

[5] L. Chettri and R. Bera, "A comprehensive survey on Internet of Things (IoT) toward 5G wireless systems," *IEEE Internet of Things Journal*, vol. 7, no. 1, pp. 16–32, 2019.

[6] S. Dang, O. Amin, B. Shihada, and M.-S. Alouini, "What should 6G be?" *Nature Electronics*, vol. 3, no. 1, pp. 20–29, 2020.

[7] M. Latva-aho, K. Leppänen *et al.*, "Key drivers and research challenges for 6G ubiquitous wireless intelligence," 2019.

[8] W. Saad, M. Bennis, and M. Chen, "A vision of 6G wireless systems: Applications, trends, technologies, and open research problems," *IEEE network*, vol. 34, no. 3, pp. 134–142, 2019.

[9] W. Tong and P. Zhu, *6G: The Next Horizon, From Connected People and Things to Connected Intelligence*. Cambridge University Press, 2021.

[10] J. Beas, G. Castanon, I. Aldaya, A. Aragón-Zavala, and G. Campuzano, "Millimeter-wave frequency radio over fiber systems: a survey," *IEEE Communications surveys & tutorials*, vol. 15, no. 4, pp. 1593–1619, 2013.

[11] C. Lim, Y. Tian, C. Ranaweera, T. A. Nirmalathas, E. Wong, and K.-L. Lee, "Evo-

lution of radio-over-fiber technology," *Journal of Lightwave Technology*, vol. 37, no. 6, pp. 1647–1656, 2019.

[12] D. Novak, R. B. Waterhouse, A. Nirmalathas, C. Lim, P. A. Gamage, T. R. Clark, M. L. Dennis, and J. A. Nanzer, "Radio-over-fiber technologies for emerging wireless systems," *IEEE Journal of Quantum Electronics*, vol. 52, no. 1, pp. 1–11, 2015.

[13] A. Bilal, A. Quddious, M. Antoniades, A. Kanno, P. Dat, K. Inagaki, T. Kawanishi, and S. Iezekiel, "5G-NR Radio-and Power-over-Fiber System Employing Multicore Fiber for Reconfigurable Metasurface Antenna Beam Steering," *Journal of Lightwave Technology*, 2023.

[14] R. M. Borges, L. A. M. Pereira, H. R. D. Filgueiras, A. C. Ferreira, M. S. B. Cunha, E. R. Neto, D. H. Spadoti, L. L. Mendes, and A. Cerqueira, "DSP-based flexible-waveform and multi-application 5g fiber-wireless system," *Journal of Lightwave Technology*, vol. 38, no. 3, pp. 642–653, 2019.

[15] H. R. D. Filgueiras, E. S. Lima, M. S. B. Cunha, C. H. D. S. Lopes, L. C. De Souza, R. M. Borges, L. A. M. Pereira, T. H. Brandão, T. P. V. Andrade, L. C. Alexandre *et al.*, "Wireless and optical convergent access technologies toward 6G," *IEEE Access*, vol. 11, pp. 9232–9259, 2023.

[16] J. P. Santacruz, "Analog Radio-over-Fiber for 5G/6G Millimeter-Wave Communications," *Eindhoven University of Technology (TU/e)*, 2022.

[17] L. Feng, R. Q. Hu, J. Wang, P. Xu, and Y. Qian, "Applying VLC in 5G networks: Architectures and key technologies," *IEEE Network*, vol. 30, no. 6, pp. 77–83, 2016.

[18] G. Gui, M. Liu, F. Tang, N. Kato, and F. Adachi, "6G: Opening new horizons for integration of comfort, security, and intelligence," *IEEE Wireless Communications*, vol. 27, no. 5, pp. 126–132, 2020.

[19] P. H. Pathak, X. Feng, P. Hu, and P. Mohapatra, "Visible light communication, networking, and sensing: A survey, potential and challenges," *IEEE communications surveys & tutorials*, vol. 17, no. 4, pp. 2047–2077, 2015.

[20] A. Pärssinen, M.-S. Alouini, M. Berg, T. Kürner, P. Kyösti, M. E. Leinonen, M. Matinmikko-Blue, E. McCune, U. Pfeiffer, and P. Wambacq, "White paper on RF enabling 6G: opportunities and challenges from technology to spectrum," 2021.

[21] A. R. Ndjiongue and H. C. Ferreira, "An overview of outdoor visible light communications," *Transactions on Emerging Telecommunications Technologies*,

vol. 29, no. 7, p. e3448, 2018.

[22] H. Farahneh, F. Hussian, and X. Fernando, "De-noising scheme for vlc-based v2v systems; a machine learning approach," *Procedia Computer Science*, vol. 171, pp. 2167–2176, 2020.

[23] H. Farahneh, S. M. Kamruzzaman, and X. Fernando, "Differential receiver as a denoising scheme to improve the performance of V2V-VLC systems," in *2018 IEEE international conference on communications workshops (ICC Workshops)*. IEEE, 2018, pp. 1–6.

[24] M. S. Islim, S. Videv, M. Safari, E. Xie, J. J. McKendry, E. Gu, M. D. Dawson, and H. Haas, "The impact of solar irradiance on visible light communications," *Journal of Lightwave Technology*, vol. 36, no. 12, pp. 2376–2386, 2018.

[25] H. C. Ferreira, H. Grove, O. Hooijen, and A. H. Vinck, "Power line communications: an overview," *Proceedings of IEEE. AFRICON'96*, vol. 2, pp. 558–563, 1996.

[26] A. Majumder *et al.*, "Power line communications," *IEEE potentials*, vol. 23, no. 4, pp. 4–8, 2004.

[27] G. Mendelson, "All you need to know about Power over Ethernet (PoE) and the IEEE 802.3 af Standard," *Internet Citation,[Online] Jun*, p. 13, 2004.

[28] K. Hafsi, D. Genon-Catalot, J.-M. Thiriet, and O. Lefevre, "DC building management system with IEEE 802.3 bt standard," in *2021 IEEE 22nd International Conference on High Performance Switching and Routing (HPSR)*. IEEE, 2021, pp. 1–8.

[29] M. Matsuura, "Power-over-fiber using double-clad fibers," *Journal of Lightwave Technology*, vol. 40, no. 10, pp. 3187–3196, 2022.

[30] J. D. L. Cardona, P. C. Lallana, R. Altuna, A. Fresno-Hernández, X. Barreiro, and C. Vázquez, "Optically feeding 1.75 W with 100 m MMF in efficient C-RAN front-hauls with sleep modes," *Journal of Lightwave Technology*, vol. 39, no. 24, pp. 7948–7955, 2021.

[31] C. Budelmann, "Opto-electronic sensor network powered over fiber for harsh industrial applications," *IEEE Transactions on Industrial Electronics*, vol. 65, no. 2, pp. 1170–1177, 2017.

[32] Werthen *et al.*, "Power over fiber: a review of replacing copper by fiber in critical applications," *Optical Technologies for Arming, Safing, Fuzing, and Firing*, vol. 5871, pp. 85–90, 2005.

[33] M. Matsuura, H. Nomoto, H. Mamiya, T. Higuchi, D. Masson, and S. Fafard,

"Over 40-w electric power and optical data transmission using an optical fiber," *IEEE Transactions on Power Electronics*, vol. 36, no. 4, pp. 4532–4539, 2020.

[34] F. M. Al-Zubaidi, J. L. Cardona, D. S. Montero, and C. Vazquez, "Optically powered radio-over-fiber systems in support of 5G cellular networks and IoT," *Journal of Lightwave Technology*, vol. 39, no. 13, pp. 4262–4269, 2021.

[35] H. Yang, D. Peng, Y. Qin, J. Li, M. Xiang, O. Xu, and S. Fu, "10-W power light co-transmission with optically carried 5G NR signal over standard single-mode fiber," *Optics Letters*, vol. 46, no. 20, pp. 5116–5119, 2021.

[36] J. D. López-Cardona, R. Altuna, D. S. Montero, and C. Vázquez, "Power over fiber in C-RAN with low power sleep mode remote nodes using SMF," *Journal of Lightwave Technology*, vol. 39, no. 15, pp. 4951–4957, 2021.

[37] L. C. de Souza, E. S. Lima, and A. C. S. Junior, "Implementation of a full optically-powered 5G NR fiber-wireless system," *IEEE Photonics Journal*, vol. 14, no. 1, pp. 1–8, 2022.

[38] J. D. López-Cardona, C. Vázquez, D. S. Montero, and P. C. Lallana, "Remote optical powering using fiber optics in hazardous environments," *Journal of Lightwave Technology*, vol. 36, no. 3, pp. 748–754, 2017.

[39] H. Kuboki and M. Matsuura, "Optically powered radio-over-fiber system based on center-and offset-launching techniques using a conventional multimode fiber," *Optics Letters*, vol. 43, no. 5, pp. 1067–1070, 2018.

[40] D. Wake, A. Nkansah, N. J. Gomes, C. Lethien, C. Sion, and J.-P. Vilcot, "Optically powered remote units for radio-over-fiber systems," *Journal of Lightwave Technology*, vol. 26, no. 15, pp. 2484–2491, 2008.

[41] L. C. Souza *et al.*, "Optically-powered wireless sensor nodes towards industrial Internet of Things," *Sensors*, vol. 22, no. 1, p. 57, 2021.

[42] J. D. López-Cardona, D. S. Montero, and C. Vázquez, "Smart remote nodes fed by power over fiber in Internet of Things applications," *IEEE Sensors Journal*, vol. 19, no. 17, pp. 7328–7334, 2019.

[43] C. Lethien, D. Wake, B. Verbeke, J.-P. Vilcot, C. Loyez, M. Zegaoui, N. Gomes, N. Rolland, and P.-A. Rolland, "Energy-autonomous picocell remote antenna unit for radio-over-fiber system using the multiservices concept," *IEEE Photonics Technology Letters*, vol. 24, no. 8, pp. 649–651, 2012.

[44] H. J. Lee, P. J. Ker, M. Z. Jamaludin, S. Isaac, and F. Halim, "Power-over-fiber for internet of thing devices," *Journal of Energy and Environment*, 2020.

[45] F. R. Bassan, J. B. Rosolem, C. Floridia, B. N. Aires, R. Peres, J. F. Aprea,

C. A. M. Nascimento, and F. Fruett, "Power-over-fiber LPIT for voltage and current measurements in the medium voltage distribution networks," *Sensors*, vol. 21, no. 2, p. 547, 2021.

[46] M. Matsuura, N. Tajima, H. Nomoto, and D. Kamiyama, "150-W power-over-fiber using double-clad fibers," *Journal of Lightwave Technology*, vol. 38, no. 2, pp. 401–408, 2019.

[47] J. Sato and M. Matsuura, "Radio-over-fiber transmission with optical power supply using a double-clad fiber," in *OptoElectronics and Communications Conference and Photonics in Switching*. Optica Publishing Group, 2013, p. TuPO_8.

[48] M. Matsuura, H. Furugori, and J. Sato, "60 w power-over-fiber feed using double-clad fibers for radio-over-fiber systems with optically powered remote antenna units," *Optics letters*, vol. 40, no. 23, pp. 5598–5601, 2015.

[49] M. Matsuura and J. Sato, "Bidirectional radio-over-fiber systems using double-clad fibers for optically powered remote antenna units," *IEEE Photonics Journal*, vol. 7, no. 1, pp. 1–9, 2014.

[50] H. Yang, S. Wang, D. Peng, Y. Qin, and S. Fu, "Optically powered 5G WDM fronthaul network with weakly-coupled multicore fiber," *Optics Express*, vol. 30, no. 11, pp. 19 795–19 804, 2022.

[51] J. D. López-Cardona, S. Rommel, E. Grivas, D. S. Montero, M. Dubov, D. Kritharidis, I. Tafur-Monroy, and C. Vazquez, "Power-over-fiber in a 10 km long multicore fiber link within a 5G fronthaul scenario," *Optics Letters*, vol. 46, no. 21, pp. 5348–5351, 2021.

[52] T. Umezawa, P. T. Dat, K. Kashima, A. Kanno, N. Yamamoto, and T. Kawanishi, "100-ghz radio and power over fiber transmission through multicore fiber using optical-to-radio converter," *Journal of Lightwave Technology*, vol. 36, no. 2, pp. 617–623, 2018.

[53] F. X. Daiminger, F. Dorsch, and D. Lorenzen, "High-power laser diodes, laser diode modules, and their applications," in *Laser Optics' 98: Solid State Lasers*, vol. 3682. SPIE, 1998, pp. 13–23.

[54] M. Peters, V. Rossin, M. Everett, and E. Zucker, "High-power high-efficiency laser diodes at JDSU," in *High-Power Diode Laser Technology and Applications V*, vol. 6456. SPIE, 2007, pp. 141–151.

[55] R. D. Diehl, *High-power diode lasers: fundamentals, technology, applications*. Springer Science & Business Media, 2000, vol. 78.

[56] O. Svelto, D. C. Hanna *et al.*, *Principles of lasers*. Springer, 2010, vol. 1.

[57] R. Iffländer, *Solid-state lasers for materials processing: fundamental relations and technical realizations*. Springer Science & Business Media, 2001, vol. 77.

[58] P. Crump, G. Erbert, H. Wenzel, C. Frevert, C. M. Schultz, K.-H. Hasler, R. Staske, B. Sumpf, A. Maassdorf, F. Bugge *et al.*, "Efficient high-power laser diodes," *IEEE Journal of Selected Topics in Quantum Electronics*, vol. 19, no. 4, pp. 1 501 211–1 501 211, 2013.

[59] W. Koechner and M. Bass, *Solid-state lasers: a graduate text*. Springer Science & Business Media, 2006.

[60] S. Babani, A. Bature, M. Faruk, and N. Dankadai, "Comparative study between fiber optic and copper in communication link," *Int. J. Tech. Res. Appl*, vol. 2, no. 2, pp. 59–63, 2014.

[61] G. Keiser, *Optical fiber communications*. McGraw-Hill New York, 2000, vol. 2.

[62] C. Vázquez, J. D. López-Cardona, P. C. Lallana, D. S. Montero, F. M. A. Al-Zubaidi, S. Pérez-Prieto, and I. P. Garcilópez, "Multicore fiber scenarios supporting power over fiber in radio over fiber systems," *IEEE Access*, vol. 7, pp. 158 409–158 418, 2019.

[63] J. A. J. Ribeiro, "Comunicações ópticas, 4a edição," *São Paulo: Editora Érica*, 2009.

[64] A. Méndez and T. F. Morse, *Specialty optical fibers handbook*. Elsevier, 2011.

[65] S. Wang, H. Yang, Y. Qin, D. Peng, and S. Fu, "Power-over-fiber in support of 5G NR fronthaul: Space division multiplexing versus wavelength division multiplexing," *Journal of Lightwave Technology*, vol. 40, no. 13, pp. 4169–4177, 2022.

[66] M. Matsuura, "Recent advancement in power-over-fiber technologies," in *Photonics*, vol. 8, no. 8. MDPI, 2021, p. 335.

[67] T. C. Banwell, R. C. Estes, L. A. Reith, P. W. Shumate, and E. Vogel, "Powering the fiber loop optically-a cost analysis," *Journal of lightwave technology*, vol. 11, no. 3, pp. 481–494, 1993.

[68] R. Pena and C. Algora, "Semiconductor materials for photovoltaic converters applied to power-by-light systems," in *Conference on Electron Devices, 2005 Spanish*. IEEE, 2005, pp. 291–294.

[69] M. Dumke, G. Heiserich, S. Franke, L. Schulz, and L. Overmeyer, "Power transmission by optical fibers for component inherent communication," *Journal of Systemics, Cybernetics and Informatics*, vol. 8, no. 1, pp. 55–60, 2010.

[70] M. R. Islam, A. Mahfuz-Ur-Rahman, K. M. Muttaqi, and D. Sutanto, "State-of-the-art of the medium-voltage power converter technologies for grid integration of solar photovoltaic power plants," *IEEE Transactions on Energy Conversion*, vol. 34, no. 1, pp. 372–384, 2018.

[71] T. Koonen, "Indoor optical wireless systems: technology, trends, and applications," *Journal of Lightwave Technology*, vol. 36, no. 8, pp. 1459–1467, 2017.

[72] H. Cao, R. Chriki, S. Bittner, A. A. Friesem, and N. Davidson, "Complex lasers with controllable coherence," *Nature Reviews Physics*, vol. 1, no. 2, pp. 156–168, 2019.

[73] J. M. Kahn and J. R. Barry, "Wireless infrared communications," *Proceedings of the IEEE*, vol. 85, no. 2, pp. 265–298, 1997.

[74] "3GPP TS 38.141-1. Base Station (BS) conformance testing, Part 1: Conducted conformance testing, Release 18." 2023.